


RESEARCH ARTICLE OPEN ACCESS

The Type VI Secretion System of *Sinorhizobium fredii* USDA257 Is Required for Successful Nodulation With *Glycine max* cv Pekin

Pedro José Reyes-Pérez¹ | Irene Jiménez-Guerrero¹ | Ana Sánchez-Reina¹ | Cristina Civantos¹ |
Natalia Moreno-de Castro¹ | Francisco Javier Ollero¹ | Jacinto Gandullo² | Patricia Bernal¹ | Francisco Pérez-Montaño¹ 

¹Departamento de Microbiología, Facultad de Biología, Universidad de Sevilla, Sevilla, Spain | ²Departamento de Biología Vegetal y Ecología, Facultad de Biología, Universidad de Sevilla, Sevilla, Spain

Correspondence: Irene Jiménez-Guerrero (ijimgue@us.es) | Patricia Bernal (pbernal@us.es) | Francisco Pérez-Montaño (fperezm@us.es)

Received: 4 December 2024 | **Revised:** 29 January 2025 | **Accepted:** 3 February 2025

Funding: This work was funded by grants from the State Subprogram for Knowledge Generation from the Spanish Minister of Science, Innovation and Universities (MICIU), the Spanish State Research Agency (AEI) and the European Union (UE) (MICIU/AEI/[10.13039/501100011033](https://doi.org/10.13039/501100011033)).

Keywords: competition | legume | nodulation | rhizobium | symbiosis | T6SS effectors | type VI secretion system

ABSTRACT

The symbiotic relationship between rhizobia and legumes is critical for sustainable agriculture and has important economic and environmental implications. In this intricate process, rhizobial bacteria colonise plant roots and induce the formation of specialised plant organs, the nodules. Within these structures, rhizobia fix environmental nitrogen into ammonia, significantly reducing the demand for synthetic fertilisers. Multiple bacterial secretion systems (TXSS, Type X Secretion System) are involved in establishing this symbiosis, with T3SS being the most studied. While the Type 6 Secretion System (T6SS) is known as a “nanoweapon” commonly used by diderm (formerly gram-negative) bacteria for inter-bacterial competition and potentially manipulating eukaryotic cells, its precise role in legume symbiosis remains unclear. *Sinorhizobium fredii* USDA257, a fast-growing rhizobial strain capable of nodulating diverse legume plants, possesses a single T6SS cluster containing genes encoding structural components and potential effectors that could target plant cells and/or act as effector-immunity pairs. Our research reveals that this T6SS can be induced in nutrient-limited conditions and, more importantly, is essential for successful nodulation and competitive colonisation of *Glycine max* cv Pekin. Although the system did not demonstrate effectiveness in eliminating competing bacteria in vitro, its active presence within root nodules suggests a sophisticated role in symbiotic interactions that extends beyond traditional interbacterial competition.

1 | Introduction

Rhizobia are α - and β -Proteobacteria soil-borne microorganisms frequently found on leguminous plant roots and rhizosphere. This environment is highly appropriate for rhizobia development and, eventually, they form a symbiotic relationship with the leguminous plant. The rhizosphere protects rhizobia from desiccation, extreme temperatures and light stress. At the same time, legumes supply bacteria with nutrients

exuded from the roots, including amino acids, organic acids, sugars, aromatic compounds and secondary metabolites (Walker et al. 2003). Flavonoids are secondary metabolites exuded by legume plants that initiate the molecular dialogue between them and rhizobia. This dialogue culminates with the formation of new root organs called nodules, where the bacterial reduction of atmospheric nitrogen to the most needed form (ammonia) takes place (Oldroyd et al. 2011). Therefore, when recognised by the appropriate rhizobia,

This is an open access article under the terms of the [Creative Commons Attribution-NonCommercial](https://creativecommons.org/licenses/by-nc/4.0/) License, which permits use, distribution and reproduction in any medium, provided the original work is properly cited and is not used for commercial purposes.

© 2025 The Author(s). *Microbial Biotechnology* published by John Wiley & Sons Ltd.

flavonoids induce the production of rhizobial signal molecules, called nodulation factors (Nod factors). Nod factors can be specifically recognised by legume plants, initiating the nodulation process that culminates with nodule development, its occupation and the transformation of the rhizobium into a nitrogen-fixing cell, the bacteroid (Oldroyd 2013; Zipfel and Oldroyd 2017). Besides the molecular recognition mediated by flavonoids and Nod factors, the success of the nodulation process also depends on secretion system effectors. Thus, in the last 15 years, effector proteins secreted through the rhizobial type III secretion system (T3SS) have been proven important, and in some cases essential, for the symbiotic performance of several rhizobial genera, such as *Sinorhizobium*, *Rhizobium*, *Bradyrhizobium* and *Mesorhizobium* (Jiménez-Guerrero et al. 2022, 2021; López-Baena et al. 2016). Interestingly, a novel secretion system, the type VI secretion system (T6SS), has been described over the past two decades, and may play a complementary role to the effects observed by T3SS effectors. This machinery was first identified in *Rhizobium leguminosarum* (Bladergroen et al. 2003), although the term T6SS was not established until 2006 when the T6SS of *Vibrio cholerae* and *Pseudomonas aeruginosa* were simultaneously characterised (Mougous et al. 2006; Pukatzki et al. 2006). The T6SS is present in ca. 25% of diderm (formerly gram-negative) bacteria, mainly in the Pseudomonadota (formerly Proteobacteria) phylum, where the α -, β - and γ -proteobacteria classes are included (Boyer et al. 2009). Generally, this system secretes effectors/toxins into prokaryotic cells, playing a critical role in interbacterial competition (Ho et al. 2014). However, some T6SS effectors target eukaryotic cells and can manipulate the host during an infective process (Hachani et al. 2016).

The specific role of T6SS effectors in rhizobial symbiosis is understudied, although recent work suggests that these proteins could exert neutral, positive, or negative effects, depending on the symbiotic pair. Thus, it has been reported that the T6SS of *Paraburkholderia phymatum* and *Azorhizobium caulinodans* do not appear to be directly implicated in the symbiotic effectiveness between these rhizobia and the legumes *Vigna unguiculata* and *Sesbania rostrata*, respectively. However, both T6SSs are involved in symbiotic competitiveness against other rhizobial species for nodulation (De Campos et al. 2017; Lin et al. 2018). In contrast, in both *Rhizobium etli* Mim1 and *Bradyrhizobium* sp. LmicA16, the T6SS is required for efficient nodulation with *Phaseolus vulgaris* and *Lupinus* spp., respectively (Salinero-Lanzarote et al. 2019; Tighilt et al. 2022). In the case of *R. etli* Mim1, this system is expressed at high cell densities, in the presence of root exudates and within host-plant nodules (Salinero-Lanzarote et al. 2019). Interestingly, one of the T6SS effectors secreted by this system, Re78, is an antimicrobial toxin involved in interbacterial competition and nodule occupancy (De Sousa et al. 2023). On the contrary, *Rhizobium leguminosarum* RBL5787 is unable to form nitrogen-fixing nodules on peas (*Pisum sativum*) due to the presence of a functional T6SS (Bladergroen et al. 2003).

Structurally, the T6SS is a multiprotein complex composed of 13 main constituents. The genes encoding these proteins are grouped into genetic clusters and named *tss* (type six secretion) (Ho et al. 2014). In some cases, an additional set of genes, named *tag* genes (type six accessory genes), encodes accessory

proteins with regulation and fine-tuning functions (Aschtgen et al. 2010; Bernal et al. 2021; Hsu et al. 2009; Lin et al. 2018; Santin et al. 2018). The T6SS is structured into three main compartments: the membrane complex formed by TssJ, TssL and TssM, the baseplate and the tail, that is formed by an inner tube (Hcp), surrounded by a contractile sheath and ended in a needle-shaped tip (VrgG and PAAR). The T6SS effectors can be transported inside the tube, or connected to the tip, being released into the intracellular environment of the target cell upon sheath contraction. (Allsopp and Bernal 2023). Genes encoding effector/toxin proteins can be found within the T6SS cluster or are scattered throughout the genome. These genes are usually located downstream of those encoding VrgG, Hcp, and/or PAAR proteins. In some cases, T6SS effectors are encoded by the same gene that encodes Hcp, VrgG or PAAR proteins at the 3' end. Structural proteins with a C-terminal cytotoxic domain are commonly termed as “specialised” Hcp, VrgG or PAAR (Allsopp and Bernal 2023). Antibacterial T6SS effectors can target the cell envelope (peptidoglycan hydrolases, phospholipases and pore-forming effectors), or bacterial cytoplasm (nuclease and cofactor degrader effectors) (Allsopp and Bernal 2023; González-Magaña et al. 2022). Bacteria with a functional T6SS produce immunity proteins to protect from sister cell attacks and self-intoxication. T6SS effectors delivered into eukaryotic host cells are less widespread than antimicrobial effectors, but the few identified to date are involved in different steps of host manipulation to promote bacterial infection (Hachani et al. 2016).

Sinorhizobium fredii USDA257, hereafter USDA257, is a fast-growing rhizobium that was isolated from wild soybean (*Glycine soja*), but is also able to form nitrogen-fixing nodules in a wide variety of legume species, such as *G. max*, *S. rostrata*, *V. radiata*, *P. vulgaris*, *Cajanus cajan*, *Lotus japonicus* and *L. burtii* (Pueppke and Broughton 1999). USDA257 is one of the most versatile rhizobia, along with other strains of the same species, *S. fredii* NGR234 and *S. fredii* HH103, and is, therefore, a model organism in many laboratories. Interestingly, among these strains, only USDA257 contains both the T3SS and T6SS machinery. The T3SS of USDA257 has been extensively studied, playing a prominent role in symbiosis as well as in determining its nodulation host range (Staehelin and Krishnan 2015). In USDA257, legume recognition of T3SS effectors can exert positive (induction of nodulation) or negative (inhibition of nodulation) extreme effects, depending on the plant cultivar (Jiménez-Guerrero et al. 2022). However, the ecological and physiological functions of the T6SS are completely unknown in USDA257 in particular and in the *Sinorhizobium* genera in general.

In this study, we identified and characterised the USDA257 T6SS, which exhibits structural proteins with novel characteristics, implying an apparatus with a distinctive assembly and a definite set of T6SS effectors. We showed that USDA257 T6SS is induced in nutrient-limited media during the stationary phase of growth and, more importantly, when this strain colonises legume root nodules. Plant assays demonstrated that USDA257 utilises this protein secretion system to improve symbiotic effectiveness and competitiveness in *G. max* cv Pekin.

2 | Materials and Methods

2.1 | Bacterial Strains and Growth Conditions

Bacterial strains used in this work are listed in Table S1. Rhizobial strains used in this study were grown at 28°C on tryptone yeast (TY) medium (Beringer 1974), yeast extract mannitol (YM) medium (Vincent 1970) or minimal (MM) medium (Robertsen et al. 1981) with two different mannitol concentrations (3 or 10 g mL⁻¹, YM3/MM3 or YM10/MM10, respectively). *Agrobacterium tumefaciens* and *Pectobacterium carotovorum* strains were cultured in lysogeny broth (LB) (Lennox LB 5 g L⁻¹ NaCl) and agar (1.5% w/v) (Sambrook et al. 1989) at 28°C. Antibiotics were used at (μg mL⁻¹): carbenicillin (Cb), 100 for *Escherichia coli*, rifampicin (Rif), 50 for *S. fredii*; tetracycline (Tc), 10 for *S. fredii* and *E. coli*; kanamycin (Km), 50 for *S. fredii* and 25 for *E. coli*; ampicillin (Ap) 100 for *S. fredii* and *E. coli*; gentamycin (Gm), 10 for *A. tumefaciens*, *P. carotovorum*, *S. fredii* and *E. coli*; spectomycin (Spc), 50 for *S. fredii* and *E. coli*; piperacillin (Pip), 15 for *S. fredii* and *E. coli*. Genistein, a *Sinorhizobium fredii nod* gene-inducing flavonoid, was dissolved in ethanol at a concentration of 1 μg mL⁻¹ to obtain a final concentration of 3.7 μM.

2.2 | Construction of Plasmids and Bacterial Strains

Plasmids and primers used in this study are listed in Tables S2 and S3. To construct USDA257 *tssA* mutant, an internal fragment of this gene was amplified using primers P1 and P2, digested with *EcoRI* and *BamHI* and cloned into the pK18mob suicide vector, which was previously digested with the same enzymes, obtaining plasmid pMUS1480. This construct was employed to generate the *tssA* mutant strain in USDA257 by inserting the pMUS1480 vector into the USDA257 chromosome via single recombination at the *tssA* locus. The mutant was confirmed by Southern blot, PCR and sequencing. For Southern blot hybridization, DNA was blotted onto Hybond-N nylon membranes (Amersham, UK), and the DIG-DNA labeling method from Roche (Switzerland) was used following the manufacturer's instructions. The Southern blot results confirmed that the band hybridising with the probe was approximately 3.7 kb larger in the mutant strain than in the wild-type strain, as expected after the insertion of the 3.7 kb pMUS1480 vector (Figure S1).

To analyse the expression profile of the T6SS cluster, the promoter region of USDA257 *ppkA* gene was amplified with primers P3 and P4 (Table S3) resulting in a 575 bps fragment that was digested with *EcoRI* and *XbaI* and cloned into the *mcs* of plasmid pMP220, upstream the *lacZ* gene, using the same enzymes and obtaining plasmid pMP220::*P_{ppkA}*. The USDA257 wild-type strain was conjugated with plasmids pMP220::*P_{ppkA}* and pMP240 (de Maagd et al. 1988), which contain transcriptional fusions of the *ppkA* promoter from USDA257 and the *nodA* promoter of *R. leguminosarum*, respectively, to the *lacZ* gene. The strain carrying the pMP240 plasmid served as a positive control, whereas USDA257, containing the empty plasmid pMP220 (Spaink et al. 1987), was used as a negative control.

To study the expression of USDA257 T6SS during the symbiotic process, we constructed a strain with a dual reporter system that expressed both constitutive GFP- and T6SS-responsive mRFP (pBBR4::*P_{kan}*::*GFP-P_{ppkA}*::*mRFP*). Construction of the dual-reporter vector was performed using a previously developed system (Samal and Chatterjee 2021). The Samal and Chatterjee system is based on the pBBR1MCS-4 plasmid, in which a constitutively expressed *GFP* gene (*P_{kan}*::*GFP*) was divergently cloned into an *mRFP* gene preceded by the promoter region of the *eng* gene from *Xanthomonas* (*P_{eng}*). To construct the T6SS responsive mRFP reporter, we first removed *P_{eng}* from the original vector using *EcoRI* to produce a promoterless (*P_{w/o}*) *mRFP* gene in the control vector pBBR4::*P_{kan}*::*GFP-P_{w/o}*::*mRFP*. Then, we cloned the promoter region of the USDA257 *ppkA* gene (*P_{ppkA}*), amplified using primers P5-P6 (Table S3) at the *EcoRI* site to engineer the vector pBBR4::*P_{kan}*::*GFP-P_{ppkA}*::*mRFP*. The insertion was confirmed by PCR using primers P7-P8 and sequenced by Macrogen Inc. These vectors were transferred into the USDA257 strain to study the expression of T6SS in the nodules.

All plasmids described in this section were transferred from *E. coli* to *Sinorhizobium* strains by triparental conjugation (Simon 1984) using *E. coli* DH5α harbouring the plasmid pRK2013 as the helper strain (Figurski and Helinski 1979). Recombinant DNA techniques were performed according to the general protocols of (Sambrook et al. 1989).

For the production of the antibody against USDA257 Hcp protein, the *hcp* gene was cloned into an expression vector that allowed the production of a C-terminal 6xHis tagged protein. First, the *hcp* gene without the stop codon was amplified by PCR with primers P9 and P10 (Table S3) and cloned into the entry Gateway pDONR207 vector, which was replicated in *E. coli* DB3.1. The insertion was confirmed by PCR and sequenced using the primers P11 and P12. The fragment was then subcloned into the destination pET-DEST42 Gateway vector following the manufacturer's instructions (Invitrogen, USA). Then, the generated plasmid pET42-*hcp* was transferred to *E. coli* BL21 (DE3) by transformation (Sambrook et al. 1989) for protein expression.

2.3 | Bioinformatical Analysis

Sequences of 160 TssB proteins from 153 strains, belonging to 12 genera were obtained and compiled using the BLASTp tool from the NCBI website (Table S4; Boratyn et al. 2013). Sequences were aligned using ClustalW software (Sievers et al. 2011), and the phylogenetic tree was constructed using MEGA7 (Kumar et al. 2016), applying the Maximum Likelihood algorithm and a JTT matrix model (bootstrap value = 500). The phylogenetic tree was customised using the iTOL website (Letunic and Bork 2016). Amino acid sequence searches were performed using SMART (Letunic et al. 2015) and Pfam (Finn et al. 2016). The Protein Homology/Analogy Recognition Engine (Phyre²) server was used to perform a template-based approach to predict protein structural homology (Kelley et al. 2015). An additional analysis to identify structural homologues was performed using the Foldseek algorithm (Van Kempen et al. 2024), which is a structural

alignment tool based on a structural protein alphabet of tertiary interactions that operates using predicted models from the AlphaFold database (Abramson et al. 2024). The PSORTb server was used to predict the subcellular locations of the proteins (Yu et al. 2010). Conserved domains to identify orphan effector genes were identified using the Batch CD-Search Tool from the NCBI website using the VgrG, Hcp, PAAR, MIX, FIX, RIX, and PIX queries. Linear comparisons of multiple genomic T6SS loci (*vgrG* regions) were performed using clinker and clustermap.js (Gilchrist and Chooi 2021).

2.4 | β -Galactosidase Assays

Overnight cultures of *S. fredii* strains carrying the pMP220 plasmid and derived pMP220::P_{ppkA} and pMP240 were diluted to a final turbidity (A₆₀₀) of 0.01 in fresh medium containing tetracycline, and cultures were grown at 28°C and 180 rpm. At different time points, aliquots were taken to measure β -galactosidase activity in permeabilized whole cells, as described by (Zaat et al. 1987). Units of β -galactosidase activity were calculated according to the method described by Miller (1972). At least three independent assays were performed for each case, and the standard errors of the mean were calculated.

2.5 | RNA Extraction and qRT-PCR Experiments

Total RNA was isolated using a High Pure RNA Isolation Kit (Roche, Switzerland), according to the manufacturer's instructions. Verification of the amount and quality of total RNA samples was carried out using a Nanodrop 1000 spectrophotometer (Thermo Scientific, USA) and a Qubit 2.0 Fluorometer (Invitrogen, USA). Four independent total RNA extractions were performed for each condition. The (DNA-free) RNA was reverse transcribed into cDNA using the PrimeScript RT reagent Kit with gDNA Eraser (Takara, Japan). Quantitative PCR was performed using a LightCycler 480 (Roche, Switzerland) with the following conditions: 95°C for 10 min; 95°C for 30 s; 50°C for 30 s; 72°C for 20 s; 40 cycles, followed by a melting curve profile from 60°C to 95°C to verify the specificity of the reaction. The USDA257 16S rRNA gene was used as an internal control to normalise gene expression. The fold-changes in four biological samples with three technical replicates for each condition were obtained using the $\Delta\Delta C_t$ method (Pfaffl 2001). The selected genes and primers (P13–P16) are listed in Table S3.

2.6 | *S. fredii* Hcp Antibody Production

The *E. coli* BL21(DE3) strain carrying the plasmid pET42-*hcp* was inoculated in 5 mL of LB supplemented with ampicillin and incubated overnight at 37°C and 200 rpm. The culture was then transferred to 200 mL of fresh medium and incubated under the same conditions. When OD_{600nm} reached 0.6, protein expression was induced with 1 mM isopropyl β -D-1-thiogalactopyranoside (IPTG). The cultures were then grown for 4 h at 37°C and 200 rpm. Cells were harvested by centrifugation (5,000 g, 20 min, 4°C) and the pellet was resuspended

in a buffer containing 50 mM Tris-HCl (pH 7.5), 250 mM NaCl, 10 mM imidazole, 1 mg/mL lysozyme and a Protease Inhibitor Cocktail used following the manufacturer's instructions (Sigma-Aldrich, USA). The suspension was incubated for 30 min at RT and sonicated on ice five times for 30 s, with 30 s cooling intervals between sonication treatments. Cell debris was eliminated by centrifugation (10,000 g, 30 min, 4°C). The clarified lysate was filtered with a 0.45 μ m filter and incubated in a column containing 2.5 mL of Ni-Sepharose resin (Protino Ni-NTA, Macherey-Nagel, Duren, Germany). This column was previously equilibrated with 10 volumes of NPI buffer (50 mM NaH₂PO₄, 300 mM NaCl, 10 mM imidazole), allowing the binding of His-tagged Hcp to Protino Ni-NTA agarose. The column was washed with 10 volumes of buffer NPI containing 100 mM imidazole, and His-tagged Hcp protein was eluted from the resin with 1 mL of buffer NPI containing 500 mM imidazole. Following the manufacturer's instructions, His-tagged Hcp protein was washed with PBS and concentrated using an Amicon Ultra Centrifugal Filter Unit (Millipore Sigma, Burlington, MA, USA). The expression and purification of His-tagged Hcp were verified by SDS-PAGE and confirmed by western blotting using a His-tag monoclonal antibody (Cell Signalling Technology, USA). Polyclonal antibody production was carried out by the "Centro de Experimentación Animal Óscar Pintado" from the University of Seville (Spain) following the procedure described by (Vidal et al. 1980) (1 rabbit; 4 protein injections –500, 125, 125 and 125 μ g– and 2 bleedings).

2.7 | Purification and Analysis of Extracellular Proteins

Extracellular and intracellular proteins were recovered following the protocol described by Hachani et al. (2011), with some modifications. Briefly, 20 mL of the different rhizobial cultures grown on an orbital shaker (200 rpm) at 28°C for 48 h with an adjusted A₆₀₀ of 1 were centrifuged for 20 min at 10,000 g at 4°C. Bacterial pellets were normalised and resuspended in 200 μ L of sample buffer (62.5 mM Tris-HCl [pH 6.8], 2% SDS [w/v], 10% glycerol [v/v], 5% β -mercaptoethanol [w/v], and 0.001% bromophenol blue [w/v]). To eliminate any remaining cells in the supernatant, three additional sequential centrifugations (20 min, 10,000 g, 4°C) were performed. One volume of 1.8 mL from each culture supernatant was collected and precipitated with trichloroacetic (TCA) acid overnight at 4°C. The mixtures were centrifuged for 30 min at 16,000 g and 4°C. Dried pellets, previously washed with 90% acetone, were resuspended in the sample buffer. For immunostaining, proteins were separated on SDS 20%–4% (w/v) polyacrylamide gels (Bio-Rad, USA) and electroblotted onto Immun-Blot polyvinylidene difluoride membranes (Bio-Rad) using a Mini Trans-Blot electrophoretic transfer cell (Bio-Rad). Membranes were blocked with TBS containing 5% (w/v) milk powder and then incubated with the previously described antibody raised against USDA257 Hcp protein diluted 1:1000 in the same solution. An anti-rabbit HRP-linked antibody (Cell Signalling Technology, USA) was used as a secondary antibody, developed using HRP Immobilon Forte (Merck, Germany) according to the manufacturer's instructions, and visualised using an ImageQuant LAS 500 imaging workstation instrument (GE Healthcare, USA).

2.8 | Interbacterial Competition Assays

In vitro competition assays between USDA257 and different rhizobia and plant pathogens were performed as previously described (Civantos et al. 2024), with some modifications. Briefly, overnight bacterial cultures were washed and adjusted to an OD₆₀₀ of 1.0 in sterile PBS, and mixed at a 1:1 ratio between USDA257 as the attacker and *A. tumefaciens*, *P. carotovorum* and *S. fredii* HH103 as preys. 100 µL of the mixtures were plated on YM3 (for *A. tumefaciens* and *P. carotovorum*) or MM3 media (for *S. fredii* HH103) and incubated at 30°C for 24 or 48 h, respectively. Subsequently, the competitions were collected using an inoculating loop and resuspended in 1 mL of sterile PBS. The outcome of the competition was quantified by counting the colony-forming units (CFUs) using antibiotic selection of the input (time=0h) and output (time=24–48h). *A. tumefaciens* and *P. carotovorum* prey strains harboured the plasmid pRL662, which confers resistance to gentamicin and was used for antibiotic selection, whereas USDA257 was naturally resistant to streptomycin. Three independent biological experiments were performed.

2.9 | Plant Tests

To evaluate symbiotic effectiveness in nodulation assays, wild-type and mutant strains were grown in YM3 medium. Surface-sterilised seeds of *G. max* cv Pekin were pre-germinated and placed in sterilised Leonard jars, containing Färhaeus N-free solution (Vincent 1970). Germinated seeds were inoculated with 1 mL of bacterial culture at an OD₆₀₀ of 0.6. Growth conditions were 16 h at 26°C in the light and 8 h and 18°C in the dark, with 70% humidity. Nodulation parameters were evaluated after 6 weeks. The shoots were dried at 70°C for 48 h and then weighed. Nodulation experiments were performed three times, with five technical replicates for each treatment.

Competition experiments for nodulation (competitiveness) on *G. max* cv Pekin were performed using the parental and the T6SS mutant strains of USDA257. These bacteria were grown to 10⁹ cells mL⁻¹, and four to five Leonard jar assemblies containing two plant seedlings were inoculated with 1 mL of a mixture of bacterial competitors at ratios of 1:1, 1:10 and 10:1. Plants were grown for 6 weeks in a plant growth chamber under the growth conditions described above. To identify bacteria occupying the nodules, 100 *G. max* cv Pekin nodules from each treatment were surface sterilised by immersing them in 5% [w/v] sodium hypochlorite for 5 min, followed by five washing steps in sterilised distilled water. The effectiveness of the surface-sterilising treatment was checked by inoculating TY plates with 20-µl aliquots from the last washing step. Individual surface sterilised nodules were crushed in 30 µL of sterilised distilled water, and 20 µL aliquots were used to inoculate TY plates. Nodule occupancy was determined by assessing the ratio of differential antibiotic resistance of isolates (only rifampicin for the wild-type strain and rifampicin and kanamycin for the T6SS mutant). At least 10 colonies from each isolate were analysed to check the possibility of nodules containing both inoculants.

For nodule occupancy visualisation by fluorescence microscopy, 30-day-old *L. burtii* nodules formed in plants inoculated with

USDA257 harbouring the dual fluorescent reporter, were embedded in 6% agarose in water and sliced in thick layer sections (50 µm) using a Leica VT 1000S vibratome (Wetzlar, Germany). Sections of nodules were stained with 0.04% calcofluor and observed by using a Leica Stellaris 8 SPE Confocal Microscope (Leica Microsystems) (Jena, Germany) fluorescence microscope as previously described (Kawaharada et al. 2017). The image's contrast and intensity were adjusted using ImageJ software (Schindelin et al. 2015).

2.10 | Statistical Analysis

The statistical tests performed in this work are indicated in the figure legends and were done using Prism 8 (GraphPad, La Jolla, CA, USA).

3 | Results

3.1 | Genome-Wide Screening for T6SSs in N₂-Fixing Bacteria

A phylogenetic analysis determines the presence of a T6SS cluster in at least 160 N₂-fixing bacterial species from 13 different genera all belonging to the Phylum Pseudomonadota, including the main genera containing root-nodule-forming bacteria (Table S4). The selected species belong to the order *Hyphomicrobiales* (better known as *Rhizobiales*) from the α-Proteobacteria class and the order *Bulckholderiales* from the β-Proteobacteria class. We have included well-described *Agrobacterium* and *Pseudomonas* T6SSs to identify and locate the previously described T6SS phylogenetic groups (Bernal et al. 2018). The tree displayed in Figure 1 contains 160 TssB proteins, showing the phylogenetic distribution of selected rhizobia T6SSs. Our analysis shows that rhizobial T6SSs are distributed among the five main clades previously described (Boyer et al. 2009). Most of them, 140 (87.5%) belong to groups 3 (54, 33.75%) and 5 (86, 53.75%) (Figure 1). Group 3 contains a great variety of species from the *Ensifer* (= *Sinorhizobium*), *Rhizobium*, *Bradyrhizobium* and *Mesorhizobium* genera among others, as well as the first-discovered *P. aeruginosa* H1-T6SS (Mougous et al. 2006). Importantly for this work, The T6SS of USDA257 belongs to phylogenetic Group 3. Group 5 contains mostly *Rhizobium* and *Azorhizobium* species and includes the well-studied *A. tumefaciens* T6SS (Ma et al. 2014; Wu et al. 2008). Although phylogenetically-distance to the above-mentioned genera *Cupriavidus* and *Parabulckholderia* species can be found in both groups. Minority Groups 2 and 4 principally contain *Parabulckholderia* species (2, 1.25% each) and Group 1 (14, 9.75%) contains predominantly species of the *Methylobacterium* genus (Figure 1).

The number of T6SS clusters in a strain could range from 1 to 5. In some bacteria groups, namely *Pseudomonas*, they commonly contain 2 or 3 but in a broader group such as phytobacteria, only an estimated 7% of strains contain more than one cluster (Bernal et al. 2018, 2017). This number is even smaller among rhizobial T6SSs where most strains contain only a single T6SS cluster (Table S4; Figure 1).

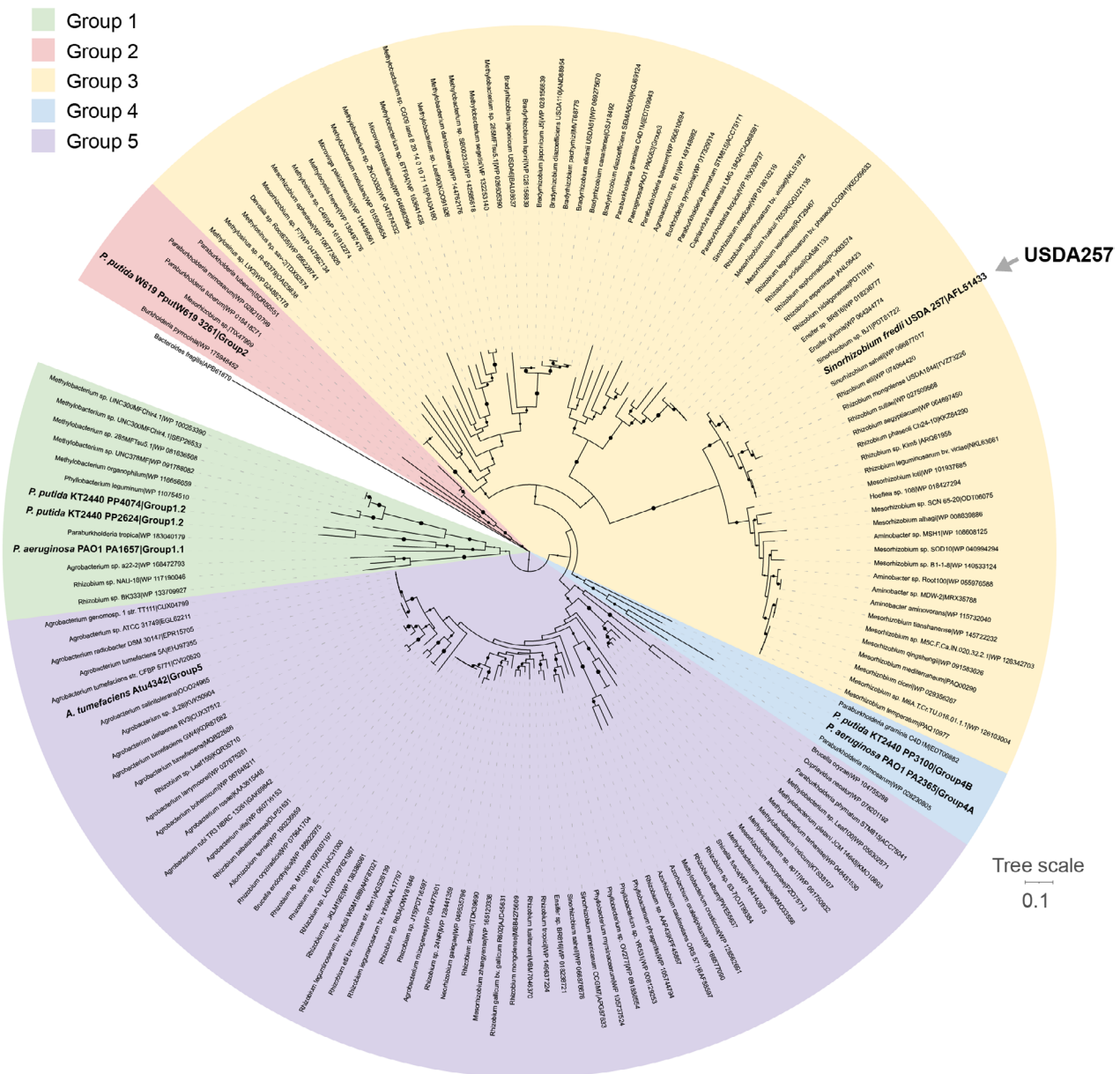


FIGURE 1 | Phylogenetic tree of T6SSs of nitrogen-fixing bacteria. Maximum likelihood tree with 500 bootstrap replicates was built with Mega 7 software for the core component protein TssB. T6SS cluster nomenclature shows the main phylogenetic clusters (Boyer et al. 2009). Branches with black circles indicate a confidence level higher than 0.75. Five phylogenetic groups are highlighted: Group 1 (green), Group 2 (red), Group 3 (yellow), Group 4 (blue) and Group 5 (purple). The bacterium of the genus *Bacteroides* represents the tree root. The position of *S. fredii* USDA257 T6SSs is marked with a grey arrow.

3.2 | The Reference Rhizobial Strain *S. fredii* USDA257 Possesses a Complete T6SS Cluster

Inspection of the USDA257 genome revealed 26 T6SS-related ORFs located in a chromosomal cluster (Figure 2A; Table S5). Thirteen genes encode the structural proteins required for a functional T6SS, including the membrane complex (TssJLM), the base plate (TssKEFG), the tail (TssBC and Hcp) and the ATPase that recycles the system (ClpV). We further identified genes encoding a previously described regulatory phosphorylation cascade (Mougous et al. 2006), including the threonine kinase/phosphatase pair (PpkA-PppA), the phosphorylation substrate (Fha) and TagF, a posttranslational repressor that regulates T6SS via Fha interaction (Lin et al. 2018).

TssJ, TssL and TssM are the core components of the T6SS membrane complex that docks the system to the cell envelope (Allsopp and Bernal 2023). According to in silico predictions, the USDA257 TssL (DotU and OmpA domains) and TssM (three IcmF domains) are anchored to the inner membrane through one and three transmembrane helices, respectively, and form a channel through the cell envelope by interaction with each other and the outer membrane lipoprotein TssJ (SciN domain) (Figure 2B). In an in-depth analysis of USDA257 T6SS components, we identified, in addition to the three core components of the membrane complex, two associated accessory proteins named TagM and TagN (Figure 2B). TagM, a 821 amino acids protein, shares a certain degree of homology with both TssL and TssM (Figure 2B; Table S5; Figure S2). This protein contains a

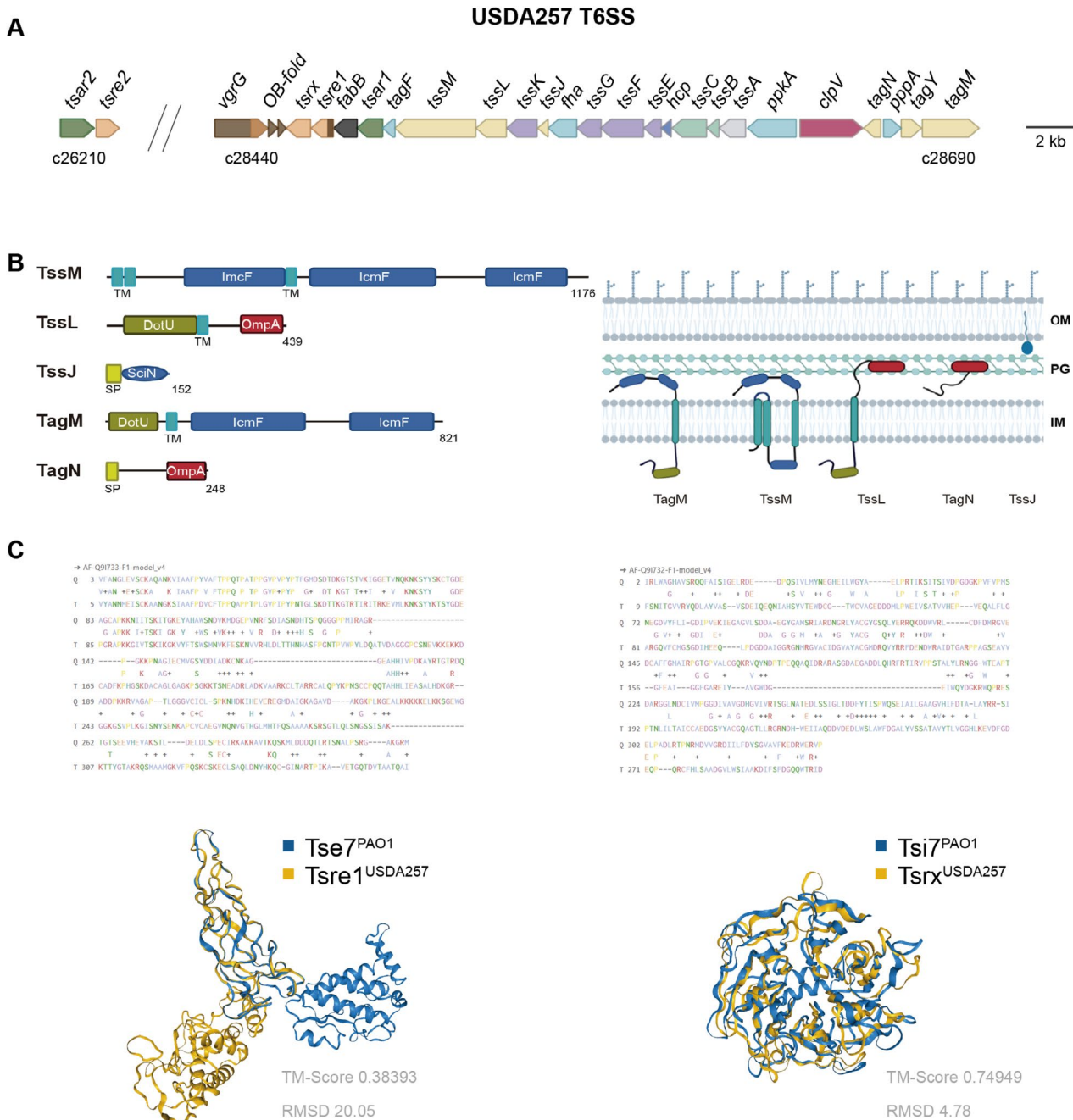


FIGURE 2 | The T6SS of *S. fredii* USDA257. (A) Organisation of the T6SS cluster of USDA257. Genes that encode the components of the membrane complex (*tssJLM*) and accessory proteins (*tagMLY*) are represented in beige. Genes coding for components of the base plate (*tssEFGK*) are shown in purple and the *tssA* gene in grey. Genes *tssB* and *tssC* encoding the contractile sheath are displayed in light green. The *hcp* gene, that encodes the protein forming the inner tube is represented in dark blue. Genes that encode regulatory proteins (*tagF*, *fha*, *ppkA* and *pppA*) are shown in light blue. The *clpV* gene which codes for the ClpV ATPase is displayed in red. Genes coding for possible effectors of the system (*tsr1*, *tsr2* and *tsrX*) are shown in light brown. Genes that encode possible adapters (*tsar1* and *tsar2*) are represented in dark green. Lately, the *vgrG* and *OB-fold* genes and the *paar* domain are displayed in dark brown. (B) Schematic representation of TssJ, TssM, TssL, TagM and TagN protein domains. Colour used to display the different domains are in brackets as follows: DotU cytosolic domain (dark green), transmembrane domain (light blue), IcmF structural domain (dark blue), OmpA peptidoglycan-binding domain (red) and signal peptide (light green). OM: Outer membrane, IM: Inner membrane, PG: Peptidoglycan layer. (C) Sequence similarities and structural alignments as predicted by AlphaFold including RMSD values and TM-scores of Tse7-Tsr1 and Tsi7-TsrX pairs. *P. aeruginosa* PAO1 proteins are displayed in blue and *S. fredii* USDA257 proteins in yellow.

cytosolic DotU domain in the N-terminal part, a single transmembrane domain and two structural IcmF domains. Its transmembrane domain and the absence of a specific signal peptide indicate this protein might be anchored to the inner membrane (Figure 2B). TagN, a 248 amino acids protein, contains a signal

peptide in the N-terminal end and an OmpA peptidoglycan (PG)-binding domain in the C-terminal part of the protein similarly to TssL (Figure 2B; Table S5; Figure S2). Lastly, we have identified a gene encoding an additional accessory protein we have named *tagY* (Figure 2A). TagY presents homology with

an M15 peptidase, a D-alanyl D-alanine carboxypeptidase that is involved in bacterial cell wall biosynthesis (Lessard and Walsh 1999).

3.3 | The *S. fredii* USDA257 T6SS Cluster Harbours Genes Encoding Putative Effectors

Frequently, genes encoding T6SS effectors are genetically linked to *vgrG* and *hcp* genes, which can be found within a T6SS cluster or, in different numbers, scattered through the genome. For instance, *P. aeruginosa* PAO1 genome contains 10 *vgrG* and 5 *hcp* genes (Hachani et al. 2016). The in silico study of the USDA257 genome has revealed single copies of *vrgG* and *hcp* genes in the T6SS cluster (Figure 2A). The *hcp* gene is found surrounded by the structural genes *tssC* and *tssE* and there is no evidence of genes encoding putative effectors in the *hcp* proximity. On the other hand, *vrgG* is located at the end of the cluster and genetically linked to putative T6SS effectors and adaptors, displaying a similar genetic architecture to *P. aeruginosa* PAO1 and *P. fluorescens* F113 *vrgG1b* clusters (Durán et al. 2021; Pissaridou et al. 2018). These *Pseudomonas vgrG* clusters encoded a VrgG, an oligonucleotide-binding (OB)-fold, a DUF2169 adaptor, a thiolase-like protein, a PAAR protein with a C-terminal cytotoxic domain, an immunity protein and a heat repeat-containing protein. The set of genes of PAO1 and F113 only differ in the sequence of the toxic domain and the cognate immunity pair (*P. aeruginosa* Tse7-Tsi7 and *P. fluorescens* Tfe6-Tfi6), a common characteristic of these genetic islands, previously described by Pissaridou et al. (2018). In USDA257, genes downstream *vrgG* are inverted relative to the *P. aeruginosa* and *P. fluorescens* clusters, but aside from this inversion, the genetic organisation of the region is conserved. In this way, USDA257 contains the genes encoding VrgG, the OB-fold protein, the DUF2169 adaptor that we have named Tsar (*tsar*, type six adaptor rhizobium), followed by the thiolase-like protein, an evolved PAAR protein named Tsre1 (*tsre*, type six rhizobial effector) with a C-terminal domain of unknown function and, lastly, a protein of unknown function that we have named Tsrx (Figure 2A). According to Phyre², which predicts structures by comparison with crystalized proteins that serve as structural templates (Kelley et al. 2015), Tsrx shows structural homology with a glycoside hydrolase enzyme GH74 with a xyloglucan binding domain from *Caldicellulosiruptor lactoaceticus* 6A (69% alignment, 99.3% confidence). In addition, the predicted model of USDA257 Tsrx protein was collected from the AlphaFold database and queried using the FoldSeek tool, which predicts the structural homology based on the tertiary interactions of proteins in a sequence-independent manner (Van Kempen et al. 2024). Using this approach, Tsrx presented high structural homology with the immunity protein Tsi7 from *P. aeruginosa* PAO1 (from amino acid 2 to 340; *E*-value of 3.77e-14, Figure 2C, right panel). Foldseek also identified structural homology between Tsrx and the glycoside hydrolase enzyme previously identified using Phyre² (from amino acid 11 to 338) but with a much lower *E*-value than the homology with Tsi7 (*E*-value 1.10e-1 vs. 3.77e-14). The C-terminal domain of the evolved PAAR protein Tsre1 does not display any structural homology using Phyre². Still, it is predicted to be structurally homologous to the DNase toxin Tse7 of *P. aeruginosa* PAO1 using AlphaFold and Foldseek tools (amino acids 3 to 321, *E*-Value 5.25e-24, Figure 2C, left panel).

Moreover, we identified another Tsar adaptor (DUF2169 adaptor) and one potential orphan effector that consists of an evolved PAAR protein (Tsre2) whose genes were located separately from the main T6SS cluster (Figure 2A, left). This orphan PAAR protein lacked sequence similarity to the Tsre1 effector in its N-terminal and C-terminal domains, and Phyre² analysis revealed no structural homology with any known proteins. This putative effector protein is conserved across some *Sinorhizobium* species, including *S. americanum* and *S. sojae*, but it is absent or significantly divergent in other bacteria. Using FoldSeek, we identified a PAAR-like DUF4150 domain-containing protein from *Methylobacterium* sp. *yr596* with limited structural homology. Specifically, structural similarity was observed only in the N-terminal PAAR region (amino acids 38–168), with a statistically significant *E*-value of 1.11e-16. Interestingly, no genes encoding a putative immunity protein were found within this genetic orphan T6SS cluster.

To obtain a broader perspective of the functioning and distribution among rhizobia of the elements that vary in the *vgrG* cluster, that is, *tsre1* and *tsrx* genes, we performed a comparison of the USDA257 *vgrG* cluster across 18 representative rhizobial strains. Synteny mapping of clusters, sorted by their *vgrG* similarity, is displayed in Figure 3A, revealing sequence conservation across the entire genetic cluster. The genes encoding the VrgG and the OB-fold proteins exhibited high sequence conservation, whereas those encoding Tsre1 and Tsrx displayed the greatest variability. Curiously, the 3' end of the DUF2169 adaptor gene and the 5' end of the gene encoding the thiolase-like protein showed reduced conservation, potentially suggesting effector/toxin specificity (Figure 3A). A neighbour-joining phylogeny of the Tsre1-like and Tsrx-like proteins from these rhizobial strains grouped USDA257 with *Sinorhizobium americanum* strains CCGM7 and CFNEI 73 in both cases, whereas most Tsre1 and Tsrx *Rhizobium phaseoli* versions are distributed in two separated branches, one grouping proteins from strains R620, R650, R611, N771, N671, N261, R723 and Brasil 5, and the other one clustering proteins from strains N841, R630, N831, N931 and R744 (Figure 3B,C). Alignment of the different Tsre1 versions revealed a high degree of similarity in the N-terminal (PAAR-like) domain, whereas the C-terminal domain showed notable divergence across all versions (Figure S3). As expected, the Tsrx versions exhibited a lower degree of similarity throughout the whole protein sequence (Figure S4). Intriguingly, despite their low sequence identity, structural homology predictions using both Phyre² and Foldseek tools suggest that Tsre1-like and Tsrx-like proteins exhibit significant structural similarity across different protein variants (Table S6).

3.4 | The T6SS of *S. fredii* USDA257 Is Functional and Induced in Minimal Medium at Stationary Phase of Growth

To determine the conditions under which the T6SS of *S. fredii* USDA257 is expressed, we constructed transcriptional fusion of the promoter region of the T6SS structural operon (*ppkA*) to the promoterless *lacZ*. We measured the expression level of USDA257 T6SS structural operon by β -galactosidase assays (See Material and Methods for more details). We tested USDA257 cultures 30h post-inoculation in selected rich,

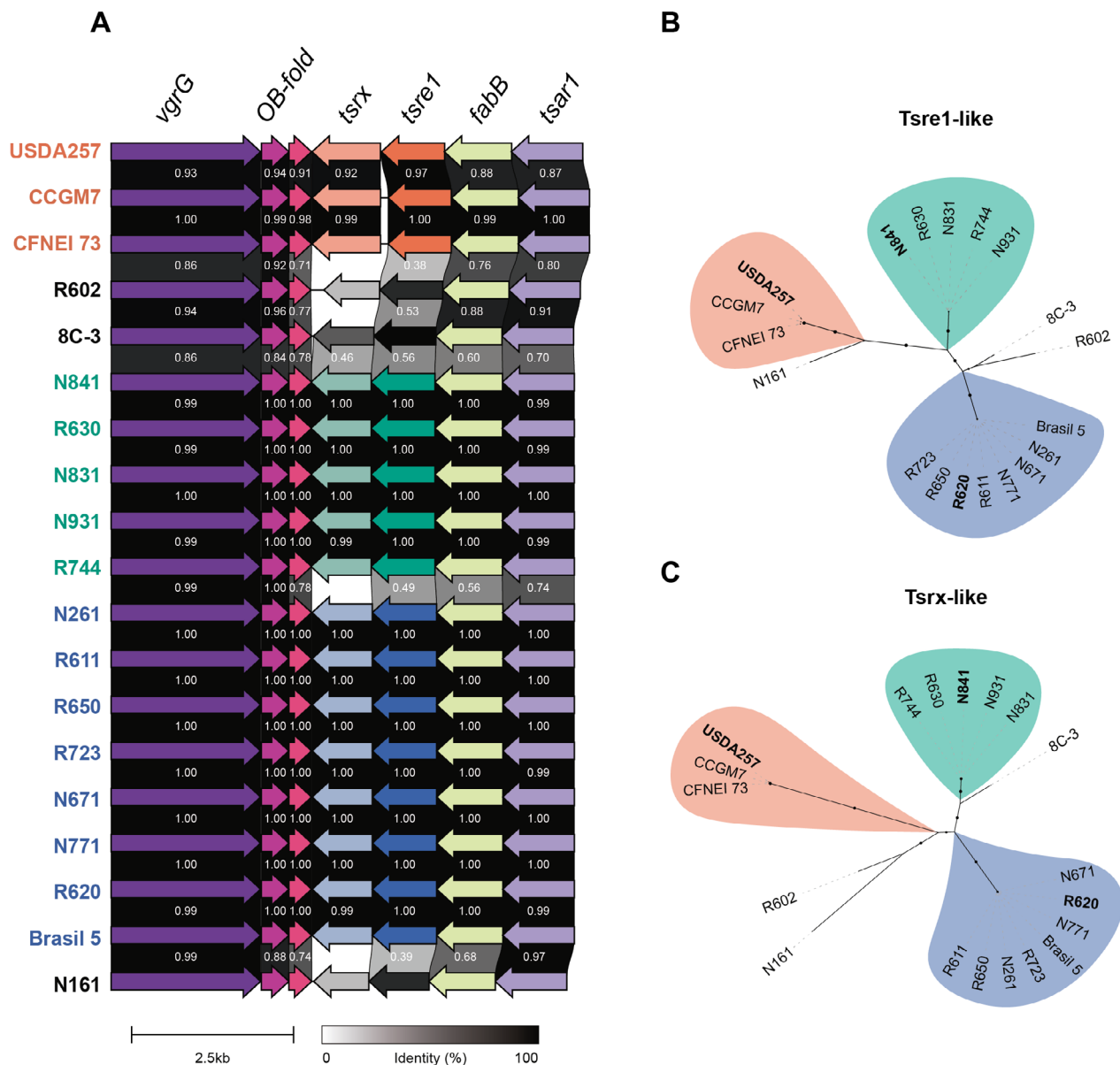


FIGURE 3 | In silico analysis of rhizobial *vrgG* clusters and putative effectors. (A) Genome sequence alignment of the *vrgG* regions demonstrated the divergence of *tsre1*-like and *tsrx*-like genes in 18 rhizobial strains using clinker & clustermap.js (Gilchrist and Chooi 2021). Clusters are sorted by homology degree with respect to the *vrgG* gene from *S. fredii* USDA257 (Blastn E value). Numbers indicate the homology degree (identity) among genes. (B and C) Neighbour-joining tree of rhizobia T6SS putative effectors with 500 bootstrap replicates. Branches with black circles indicate a confidence level higher than 0.75. Analyses of the PAAR effector (Tsre-like) (B) and the Tsrx-like proteins (C) by sequence similarity were performed by CLUSTALW in the MEGA7 software. In bold, representative Tsre1-like and Tsrx-like proteins of each branch (USDA257-group: Orange; N841-group: Green; R620-group: Blue).

standard and minimal media for growing rhizobia, that is, TY, YM, and MM respectively (Figure 4A). YM is a standard medium containing moderate amounts of yeast extract, which provides essential organic nitrogen and micronutrients. In contrast, MM is a minimal medium that exclusively contains glutamate as the nitrogen source. Both YM and MM media can be prepared using different concentrations of mannitol as the carbon source. T6SS gene expression was highest in the minimal medium MM3 (3 gL⁻¹ of mannitol) and lowest in the rich medium TY. Compared to the strain carrying the empty plasmid, gene expression was approximately 3-fold and 1.8-fold in these media, respectively (Figure 4A). To confirm these findings, we followed a complementary approach, measuring

the transcriptional activation of the USDA257 *ppkA* gene by quantitative PCR 48 h post-inoculation. qRT-PCR experiments revealed a similar transcriptional activation pattern for the USDA257 *ppkA* gene. The highest transcriptional levels were observed in the MM3 medium, demonstrating approximately 8-fold higher expression compared to cultures grown in the TY medium. (Figure 4B). To further investigate T6SS regulation, we performed β -galactosidase assays at different stages of the USDA257 growth curve, inoculating the bacterium in the MM3 medium as the inducing condition. Interestingly, the *P_{ppkA}::lacZ* fusion in the wild-type strain indicated a gradual upregulation of T6SS expression over time, with a plateau in β -galactosidase activity observed at approximately 54 h

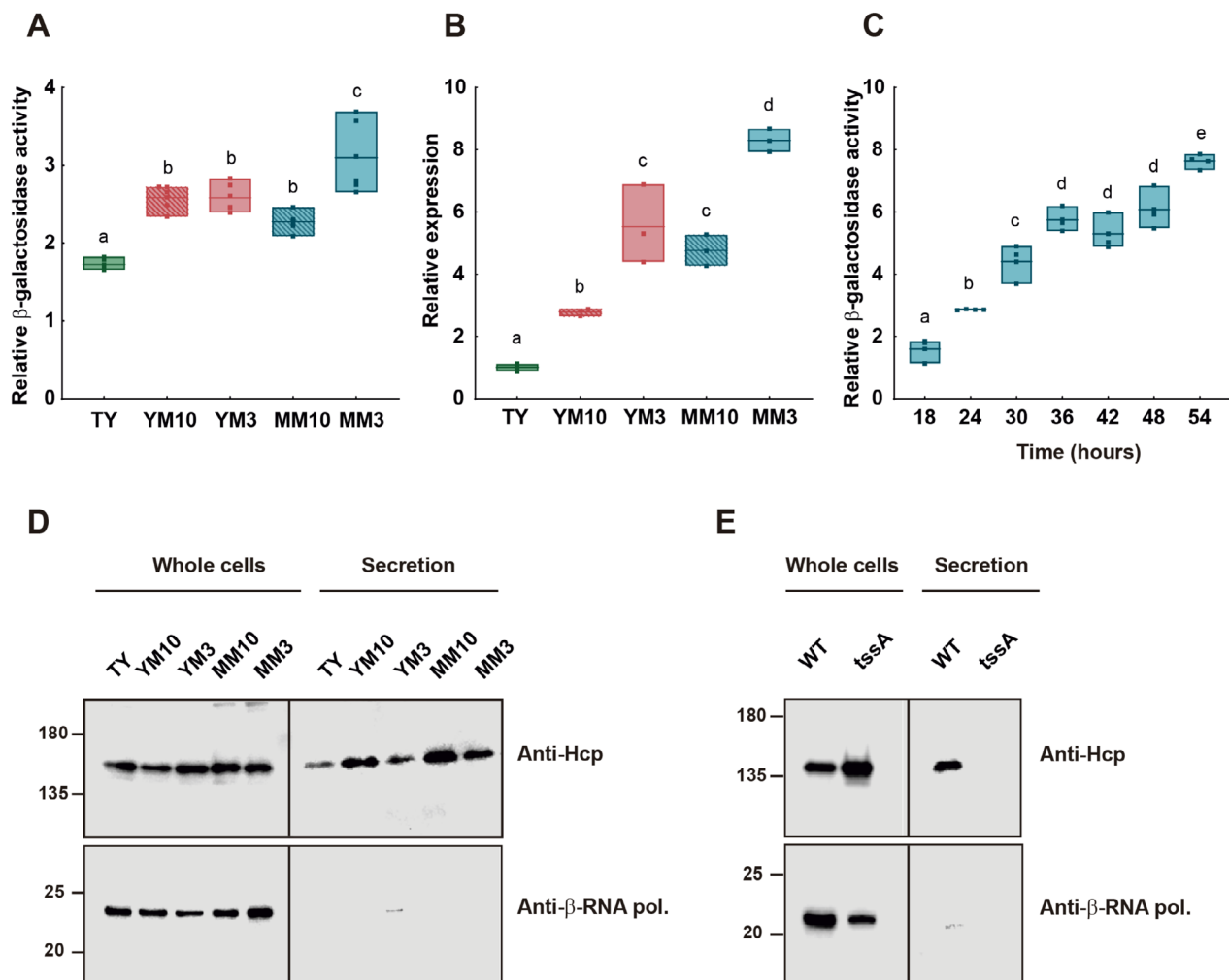


FIGURE 4 | Activation pattern and functionality of the *S. fredii* USDA257 T6SS. (A) Fold-change values of the β -galactosidase activity of USDA257 carrying a pMP220 plasmid containing the *ppkA* promoter region fused to the *lacZ* gene with respect to those values obtained by the strain carrying the empty pMP220 plasmid. The tested conditions included TY (green), YM10 (striped red), YM3 (red), MM10 (striped blue) and MM3 (blue) media evaluated 30 h post-inoculation. Expression data are presented as the mean (\pm standard deviation). Groups labelled with the same letter are not significantly different at $\alpha = 5\%$ (One-Way ANOVA with multiple comparisons, $p < 0.05$). (B) Quantitative RT-PCR analysis of the expression of the *ppkA* gene of USDA257 grown in TY (green), YM10 (striped red), YM3 (red), MM10 (striped blue) and MM3 (blue) media 48 h post-inoculation. Expression data are presented as the mean (\pm standard deviation) for three biological replicates. Groups labelled with the same letter are not significantly different at the level of $\alpha = 5\%$ (One-Way ANOVA with multiple comparisons, $p < 0.05$). (C) Fold-change values of the β -galactosidase activity of USDA257 carrying the pMP220 plasmid containing the *ppkA* promoter region fused to the *lacZ* gene with respect to those values obtained by the strain carrying the empty pMP220 plasmid. The tested condition included MM3 medium at different hours post-inoculation. Groups labelled with the same letter are not significantly different at the level of $\alpha = 5\%$ (One-Way ANOVA with multiple comparisons, $p < 0.05$). (D) Production and secretion of Hcp in the USDA257 wild-type strain grown for 48 h in rich, standard and minimal media: TY, YM10, and MM10, respectively. YM3 and MM3 represent derivatives of their corresponding media with reduced carbon source content. (E) Production and secretion of Hcp in the USDA257 wild-type and the *tssA* mutant strains grown in MM3. For both panels, the Hcp protein was detected by Western blot analysis using a specific Hcp antibody. Detection of the β -subunit of the RNA polymerase using a specific antibody was used as lysis control. “Whole cells” expression represents the intracellular protein fraction, whereas “Secretion” displays the extracellular protein fraction. The position of the molecular size marker (in kDa) is indicated.

post-inoculation. This peak represented a nearly 7-fold increase compared to the empty plasmid control (Figure 4C).

Finally, to gain insight into the potential role of the USDA257 T6SS in the early steps of the symbiotic process, β -galactosidase assays were performed in the presence of genistein, a *nod*-gene-inducing flavonoid of several *S. fredii* strains, including USDA257 (López-Baena et al. 2008; Pérez-Montaña, Jiménez-Guerrero, et al. 2014) (Figure S5). Activation of the *ppkA* promoter was measured in

MM3 medium at the stationary phase of growth, both in the presence and absence of genistein. As a control for *nod*-gene induction, a wild-type strain carrying the pMP240 plasmid was used. This plasmid harbours the conserved *nodA* promoter from *Rhizobium leguminosarum* bv. *viciae* fused to the *lacZ* reporter gene. Induction values for strains carrying the *ppkA* promoter fused to *lacZ* were comparable across all conditions (Figure S5), indicating that the T6SS operon expression is not regulated by the presence of the flavonoid genistein in the tested conditions.

The extracellular secretion of the Hcp protein into a culture medium is a hallmark for assessing the functionality of the T6SS system. Therefore, we produced a specific polyclonal antibody against USDA257 Hcp (see Section 2 for more details) to test T6SS activity in different culture media after 48 h of growth (Figure 4D). The results of these secretion assays were consistent with the transcriptomic data (Figure 4A–C). Specifically, we observed low levels of Hcp secretion in the TY medium, while significantly higher levels were detected in both minimal media.

To demonstrate that Hcp secretion was T6SS-dependent, we obtained a USDA257 *tssA* mutant strain to disable the system, since TssA is an essential component for T6SS activity. As expected, we detected Hcp in the supernatant of the wild-type strain grown in MM3 but not in the isogenic *tssA* mutant, while it was present in the cytosol of both strains (Figure 4E). Altogether, these results established that USDA257 T6SS is a functional secretion machinery, that is induced in minimal media at the stationary phase of growth.

3.5 | The T6SS of *S. fredii* USDA257 Is Required for Successful Nodulation and Competitiveness With *G. max* cv Pekin

Most bacterial T6SSs are involved in interbacterial competition. For this reason, we performed killing assays using the wild-type and a *tssA* mutant (T6SS-defective) strains of USDA257 as predators and other bacterial species (*A. tumefaciens*, *P. carotovorum* and *S. fredii* HH103) as preys. The bacteria were mixed 1:1 (predator: prey) and co-cultured on USDA257 T6SS-inducing medium for 24 and 48 h. Spots containing the competing bacteria were collected and the bacterial CFUs were determined on selective plates. As shown in Table S7, the viability of the different tested prey cells was not diminished after co-incubation with the USDA257 wild-type strain. These results indicate that USDA257 was not able to compete in a T6SS-dependent manner against other potential rhizospheric competitors as the phytopathogens *A. tumefaciens* and *P. carotovorum* or the symbiont *S. fredii* HH103 in the tested conditions (Table S7). In addition to the fact that no differences were observed between the viability of the prey cells when competing with USDA257 wild-type or the mutant strains, both wild-type and the *tssA* mutant displayed a reduced number of CFU after competition, indicating that USDA257 competes less effectively for resources than the prey cells used in these competition assays (Table S7).

To gain insight into the role and functioning of the USDA257 T6SS in vivo, the symbiotic abilities of the wild-type or its derivative *tssA* mutant strains with *G. max* cv Pekin, considered its natural host, were inspected (Figure 5). Interestingly, the number of nodules in examined plants inoculated by the *tssA* mutant was statistically lower than those obtained in plants infected by the wild-type strain (Figure 5A). Similar but not statistically significant trends were observed for both nodule fresh mass and plant-top dry mass parameters (Figure 5B,C).

The role of the T6SS in rhizobial competitiveness for nodule occupancy in *Glycine max* cv Pekin was investigated through

co-inoculation experiments between USDA257 and its *tssA* mutant at three different inoculation ratios: 1:1, 1:10, and 10:1. Six weeks post-inoculation, nodule occupancy was quantified, revealing significant competitive advantages for the wild-type strain. At the 1:1 ratio, the wild-type strain occupied 64% of nodules, substantially higher than the expected 50% if both strains had equal competitive capabilities. Similarly, at the 10:1 ratio, the wild-type strain colonised 17% of nodules, compared to the anticipated 10% (Figure 5D). These findings demonstrate that the T6SS of USDA257 is important for optimal symbiotic performance and competitive nodulation in soybean cv Pekin.

The influence of T6SS on symbiotic success points out that this protein secretion system is functional within the host plant. To investigate this, we employed in vivo confocal microscopy to monitor the USDA T6SS expression and localization of rhizobial cells during the later stages of symbiosis. Using a dual-bioreporter system with constitutive GFP and T6SS-responsive mRFP, we tracked USDA257 cells throughout the infection of *Lotus burtii* nodules. While the GFP signal provided a consistent marker for all bacterial cells, the mRFP fluorescence revealed a critical insight, the T6SS was actively expressed in all rhizobia colonising the symbiotic cells (Figure 5E). This observation demonstrates that the T6SS of USDA257 is fully operational during the invasion and establishment of nodule tissue, highlighting its potential significance in the symbiotic interaction.

4 | Discussion

Applying symbiotic rhizobia offers a cost-effective and environmentally sustainable alternative nitrogen source for plants, potentially reducing dependence on synthetic nitrogen fertilisers (Martinelli et al. 2020; Pérez-Montaño, Alías-Villegas, et al. 2014). The efficiency of symbiosis depends on various factors, including the soil, the environment, and the symbiotic pair. From the rhizobial perspective, several molecules are important in this intimate interaction, including Nod factors, extracellular polysaccharides, and protein secretion systems (López-Baena et al. 2016). Plant-interacting microbes predominantly use the T3SS to deliver protein effectors directly into host cells, facilitating infection (Feng and Zhou 2012; Jiménez-Guerrero et al. 2015). In response, plants have developed a sophisticated defence mechanism involving resistance proteins that recognise these effectors, triggering an immune response known as effector-triggered immunity, which can effectively halt bacterial invasion (Duxbury et al. 2016; Mansfield 2009; Mudgett 2005). Thus, rhizobial T3SS effectors can exert neutral, positive or negative effects on symbiosis depending on the specific repertoire of plant resistance proteins (Jiménez-Guerrero et al. 2022; Nelson and Sadowsky 2015). An additional secretion system that delivers effectors inside eukaryotic cells is the T6SS, discovered in 2006 (Mougous et al. 2006; Pukatzki et al. 2006), but research exploring its role in rhizobial symbiosis remains limited. Our study focuses on the unique T6SS cluster of *Sinorhizobium fredii* USDA257, which belongs to phylogenetic Group 3 (Figure 1), one of the most prevalent phylogenetic groups within the *Rhizobiales* order, alongside Group 5. While the T6SS of *A. tumefaciens* from phylogenetic Group 5 has been extensively characterised and found primarily involved in interbacterial competition

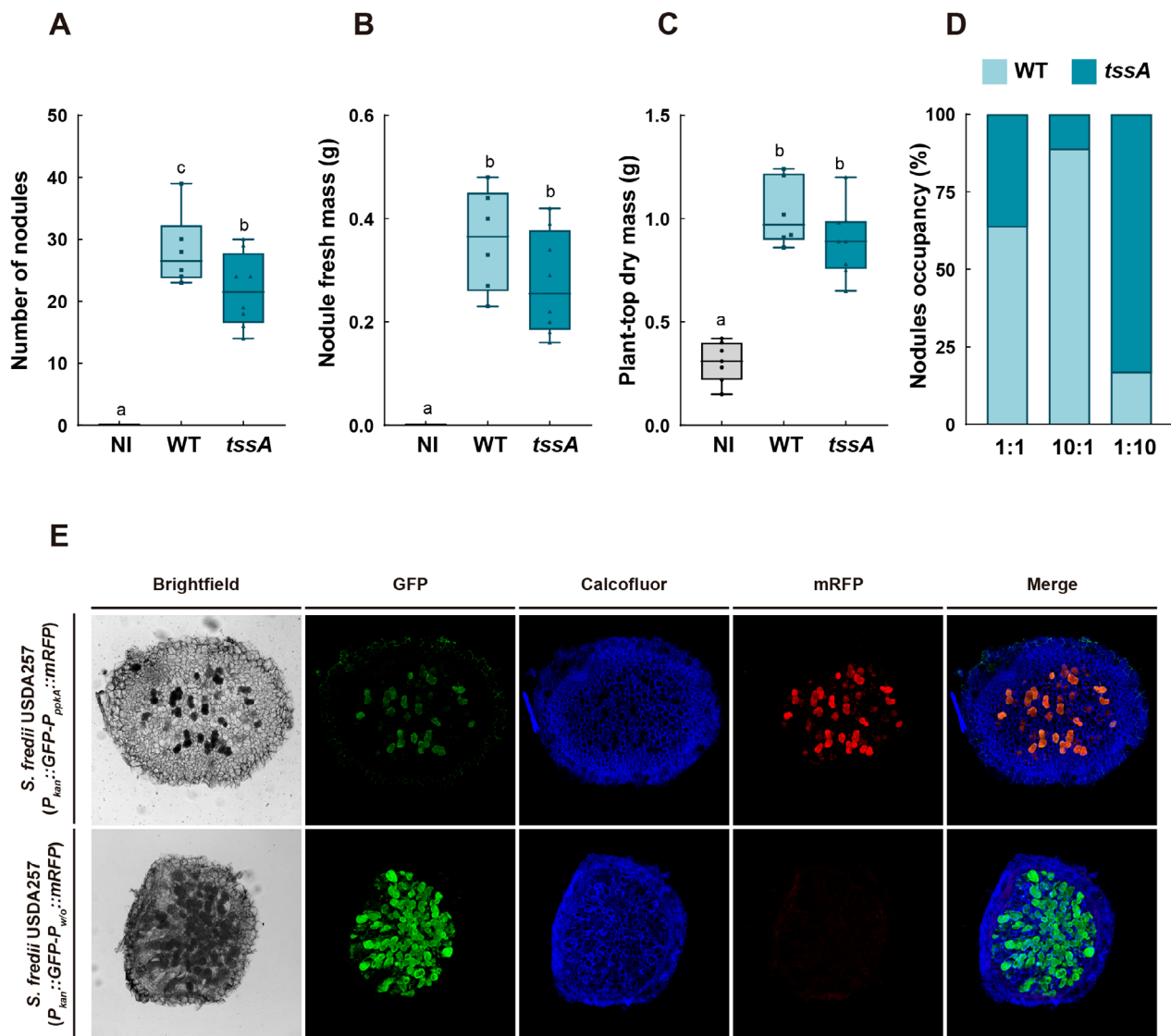


FIGURE 5 | Plant responses to inoculation with *S. fredii* USDA257 strains. (A–C) *G. max* cv Pekin responses to inoculation with different *S. fredii* USDA257 strains (WT: Light blue, *tssA*: Dark blue). Plants were evaluated 6 weeks after inoculation. NI: Non-inoculated plants (grey). Data indicated with the same letter are not significantly different at the level of $\alpha = 5\%$ (One-Way ANOVA with multiple comparisons, $p < 0.05$). (D) Competition for nodulation assays of different *S. fredii* USDA257 strains. Percentages of nodule occupancy were evaluated by co-inoculation at different ratios of both strains at 30 days post-inoculation (dpi) (WT: Light green, *tssA*: Dark green). (E) Confocal microscopy of *L. burttii* nodules 30 dpi with *S. fredii* USDA257 carrying a dual fluorescent reporter vector with or without the *ppkA* promoter region upstream of the *mRFP* gene.

(Ma et al. 2014), investigations into *Rhizobiales* Group 3 T6SS clusters are notably sparse. In fact, prior to this research, only a single T6SS cluster from *Rhizobiales* Group 3 had been examined, revealing its involvement in nodulation efficiency (Hug et al. 2021).

Our in-depth in silico analysis indicates that the genome of USDA257 contains the 13 genes coding for all core structural proteins required for a functional T6SS (Figure 2A). The set included a specialised TssL with a canonical N-terminal DotU domain and an additional C-terminal OmpA domain that it is expected to bind peptidoglycan (Figure 2B) and that have been previously identified in *P. aeruginosa* and *A. tumefaciens* among others (Aschtgen et al. 2010). Besides the canonical T6SS membrane complex proteins (TssJLM), USDA257 encodes two accessory proteins, TagM (DotU and IcmF domains) and TagN

(OmpA domain) that combine domain proteins from TssL and TssM, and are expected to be part of the membrane complex and assist with the anchoring of USDA257 T6SS to the peptidoglycan (Figure 2B). A similar protein to USDA257 TagN have been previously described in *Burkholderia pseudomallei* and *Ralstonia solanacearum* and equally consist of a ~250 amino acids protein with an N-terminal signal peptide and a C-terminal OmpA domain (Aschtgen et al. 2010). Moreover, USDA257 T6SS presents TagY with homology to an M15 peptidase and a predicted signal peptide that suggests that this protein could be anchored to the outer membrane with the C-terminal end facing the periplasm. The M15 peptidase is a D-alanyl D-alanine carboxypeptidase involved in bacterial cell wall biosynthesis and reorganisation (Hung et al. 2013; Lessard and Walsh 1999). Thus, TagY might be important for enabling the insertion of the T6SS machinery across the peptidoglycan layer. Similarly, in *Acinetobacter*

baumannii, the peptidoglycan hydrolase TagX, encoded within the T6SS cluster, is responsible for remodelling the peptidoglycan to facilitate membrane complex assembly and thus it is essential for T6SS biogenesis in this bacterium (Weber et al. 2016). The presence of these four proteins (TssL, TssM, TagM and TagN) with characteristic domains of the T6SS membrane complex (DotU, IcmF and OmpA) and the putative peptidoglycan modifier TagY reflects a special way to anchor the system to the membrane that might confer novel features to this machinery that remain to be unveiled.

T6SSs are tightly controlled by different regulatory proteins (Bernal et al. 2023; Hespanhol et al. 2023; Lin et al. 2018). A well-studied example is the kinase-phosphatase PpkA-PppA couple from *P. aeruginosa*, which mediates the system formation through a phosphorylation cascade that ends with the structural components assembly. In the USDA257 cluster, we identified not only genes encoding the PpkA-PppA regulatory proteins but also those encoding Fha and TagF proteins, which interact with the system to regulate its activity at the post-transcriptional level and are in many cases related to the PpkA-PppA cascade as seen in *P. aeruginosa* and *A. tumefaciens* (Lin et al. 2018). The presence of all these proteins in USDA257 suggests that this system may exhibit a regulation mechanism similar to that of these strains.

Genes encoding effector proteins are often found within the T6SS cluster, specifically in the *vggG* gene neighbourhood (Durand et al. 2014). In USDA257, the *tsre1* gene encodes an evolved protein with an N-terminal PAAR domain. The C-terminal domain of Tsre1 shows structural homology with a glycoside hydrolase enzyme which presents a xyloglucan binding domain able to hydrolyze the plant cell wall (Arnal et al. 2019), but also, and with higher confidence with the DNase toxin Tse7 from *P. aeruginosa* PAO1 (Figure 2C) (Pissaridou et al. 2018). The gene downstream *tsre*, *tsrx*, encodes Tsrx which possesses structural similarity to the antitoxin protein Tsi7 (Figure 2C), supporting the potential role of Tsre-Tsrx as a toxin-antitoxin pair. Intriguingly, a comparative analysis of these proteins across several rhizobial strains indicates that, despite the absence of sequence similarity among Tsre1-like or Tsrx-like proteins (Figure 3C), they consistently exhibit structural homology to Tse7 and Tsi7, respectively (Table S6). This suggests that, regardless of the specific function of these proteins, it is likely to be conserved among rhizobia. Moreover, the possibility emerges that Tsre1 and Tsrx might function as moonlighting proteins, that is, multifunctional molecules capable of performing diverse biological functions depending on cellular localization, molecular interactions, or environmental fluctuations (Jeffery 1999). Supporting this hypothesis, a recent study demonstrated the multitasking potential of thioredoxin 1 (TrxA), a protein that functions not only as a thioredoxin but also as a chaperone of the toxin TreX, translocated through the *Xenorhabdus bovienii* T6SS. Comparisons with similar toxins suggest that the chaperone role of TrxA evolved from an ancestral redox function (Dumont et al. 2024). Moreover, it has been recently proposed that moonlighting proteins may be particularly important when the symbiotic interaction becomes more intimate, that is, during the development of the symbiosome (Ma et al. 2024). Importantly, this developmental stage coincides precisely with the peak activity of USDA257 T6SS, as demonstrated by the fluorescence microscopy data in Figure 5E.

Overall, the exhaustive in silico analysis performed in this work suggests a functional T6SS of *S. fredii* USDA257, which might be involved in the interaction with host plant cells and/or with bacteria present in the plant rhizosphere. *S. fredii* USDA257 is a rhizobial species with an exceptionally broad host range, nodulating over 100 genera of legumes (Pueppke and Broughton 1999). One of the molecular keys to broaden the host range in the *Sinorhizobium* genera is the T3SS (Jiménez-Guerrero et al. 2022; Krysciak et al. 2015). However, is the USDA257 T6SS also fully functional and involved in the direct or indirect optimization of the nodulation process? According to our results, the USDA257 T6SS is expressed at the late stages of the symbiotic process (within nodules) (Figure 5E) and in nutrient-limited conditions at the stationary phase of growth (Figure 4), but not in the presence of *nod*-gene-inducing flavonoids (Figure S5). This regulation differs from that described for the rhizobial T3SS, which is assembled during the early stages of symbiosis and co-regulated with Nod factor production (López-Baena et al. 2008). The findings described for *R. etli* T6SS are largely similar to those for USDA257 T6SS. This protein secretion system is fully functional in yeast mannitol medium in stationary phase and bean nodules (Salinero-Lanzarote et al. 2019). Likewise, in other systems like *Pseudomonas putida* K1-T6SS and *E. coli*, T6SS is induced during the stationary phase of growth and activated in regulatory mutants (*retS*, *rpoS*, *rpoN* and *fleQ*) (Bernal et al., 2023; Hespanhol et al. 2023). Induction of rhizobial T6SSs in minimal media has also been reported (Salinero-Lanzarote et al. 2019). In pathogenic bacteria such as *Vibrio cholerae*, host-derived molecules like bile salts, chitin and mucilage trigger T6SS activation by inhibiting specific repressors (Bachmann et al. 2015; Borgeaud et al. 2015). No T6SS regulatory mutants have been identified in rhizobia strains, presenting an interesting avenue for future research. As described in other bacteria, the expression at high population densities suggests that the transcriptional activation of rhizobial T6SS genes may be influenced by bacterial quorum sensing (QS) (Hespanhol et al. 2023). QS is a cell-density-dependent bacterial communication system that synchronises gene expression and behaviour (Winzer and Williams 2001). This system is known to regulate T6SS gene expression in several microorganisms that interact with eukaryotic hosts, such as *Vibrio* spp. (Zheng et al. 2010), *Aeromonas hydrophila* (Khajanchi et al. 2009), *Chromobacterium violaceum* (Alves et al. 2022), *Enterobacter cloacae* (Sabag-Daigle et al. 2015) and *P. aeruginosa* (Lesic et al. 2009).

A successful symbiotic relationship can be evaluated by two key factors, symbiotic effectiveness (measured by shoot dry mass, and the number and fresh mass of nodules) and symbiotic competitiveness (percentage of nodule occupancy). Symbiotic effectiveness describes how efficiently a strain forms nodules with its host plant, while symbiotic competitiveness refers to the strain's ability to outcompete other bacteria during co-infection (Bromfield and Jones 1979). The involvement of the USDA257 T6SS in the symbiotic process has been confirmed in nodulation and competitiveness for nodule occupancy assays (Figure 5A–D). The absence of this protein secretion system reduces the formation of nodules and their relative nodule colonisation in soybeans. Thus, this protein secretion system may modulate the plant defence responses, either through effector proteins targeting the host cells or via the plant recognition of structural proteins. Positive effects of T6SS on symbiosis have been recently

reported in the systems *R. etli*-bean and *Bradyrhizobium-Lupinus*. *R. etli* Mim1 mutants defected in T6SS structural genes produced plants with lower biomass and smaller nodules compared to the wild-type strain (Salinero-Lanzarote et al. 2019). Similarly, a *Bradyrhizobium* spp. LmicA16 mutant lacking the T6SS nanostructure induced fewer nodules, resulting in smaller plants than those inoculated with the wild-type strain, and was less competitive for nodule occupancy when co-inoculated with the parental strain (Salinero-Lanzarote et al. 2019; Tighilt et al. 2022). Conversely, the first study related to T6SS and performed on rhizobia reported a negative effect of T6SS in symbiosis. Here, the insertion of a transposon in the *tssK* gene of *R. leguminosarum* RBL5787 enabled the bacterium to establish a successful symbiosis relationship with pea that was otherwise blocked (Bladergroen et al. 2003). Studies on *P. phymatum* and *A. caulinodans* revealed that the T6SSs of these strains are not directly involved in symbiotic effectiveness with their host legumes *V. unguiculata* and *S. rostrata*, respectively. Thus, nodule phenotype, size and nitrogen-fixation ability showed no differences between T6SS mutants and wildtype strains when infected individually (De Campos et al. 2017; Lin et al. 2018). However, in both cases, the T6SS enhanced the symbiotic competitiveness of *P. phymatum* and *A. caulinodans* during coinfection with a T6SS-deficient strain.

Interbacterial competition activity in vitro has been demonstrated for *P. phymatum* and *A. tumefaciens* (De Campos et al. 2017; Ma et al. 2014), but it was not found for *A. caulinodans* (Lin et al. 2018). Similarly, competition assays with USDA257 against various rhizobacteria under in vitro T6SS-inducing conditions indicate that this protein secretion system does not confer killing ability to USDA257 (Table S7), at least in the tested conditions. However, this result partially contradicts the in silico analysis of the TsrE1 effector, which suggests that this protein shares structural homology with a DNase-type toxin (Figure 2C). It cannot be excluded that the capacity to eliminate competing rhizobia may develop during the later phases of symbiosis, such as during in vivo root colonisation and infection, where this system is fully active (Figure 5). This might explain the absence of detectable toxic effects mediated by TsrE1 under in vitro laboratory conditions. Similarly, *A. tumefaciens* deploys DNase effectors as weapons for interbacterial competition in planta but not in vitro, where is lethally counterattacked by *P. aeruginosa* (Ma et al. 2014). Additional investigation is required to confirm this hypothesis in *S. fredii* USDA257.

5 | Conclusions

The ecological success of rhizobia is based on their great capacity to adapt, not only to environmental changes as free-living soil bacteria, but also to the challenges they face during root colonisation, invasion through the infection tube, and their establishment as mature nitrogen-fixing bacteroids in nodule cells. So far, studies have primarily focused on the characterisation of nodulation factors, surface polysaccharides, and the T3SS. However, our results point to a new level of specificity mediated by T6SS effectors, which optimise the symbiotic efficiency by enhancing rhizobial competitiveness during nodulation. Despite the proposed functions for some putative USDA257 T6SS effectors, future research is needed to elucidate their mechanisms and understand their specific roles in the rhizosphere and symbiosis.

Author Contributions

Pedro José Reyes-Pérez: methodology, validation, formal analysis, investigation, visualization. **Irene Jiménez-Guerrero:** conceptualization, methodology, validation, formal analysis, supervision, investigation, writing – review and editing, project administration. **Ana Sánchez-Reina:** investigation, visualization. **Cristina Civantos:** investigation, validation. **Natalia Moreno-de Castro:** investigation, validation. **Francisco Javier Ollero:** investigation, validation. **Jacinto Gandullo:** validation, supervision. **Patricia Bernal:** methodology, conceptualization, writing – review and editing, writing – original draft, funding acquisition, visualization, project administration, supervision. **Francisco Pérez-Montaño:** writing – review and editing, writing – original draft, funding acquisition, visualization, methodology, conceptualization, project administration, supervision.

Acknowledgements

P.B. and I.J.-G. are supported by the MICIU/AEI/10.13039/501100011033 Spanish agency through a Ramon y Cajal RYC2019-026551-I and a Juan de la Cierva Incorporación IJC2020-045968-I, respectively. This work was funded by two research grants from the State Subprogram for Knowledge Generation from the Spanish Minister of Science, Innovation and Universities (MICIU), the Spanish State Research Agency (AEI) and the European Union (UE) with reference PID2020-118279A-I00 awarded to F.P.-M. and PID2021-123000OB-I00 (MICIU/AEI/10.13039/501100011033) awarded to P.B.

Conflicts of Interest

The authors declare no conflicts of interest.

Data Availability Statement

The data are available within the manuscript.

References

- Abramson, J., J. Adler, J. Dunger, et al. 2024. “Accurate Structure Prediction of Biomolecular Interactions With AlphaFold 3.” *Nature* 630, no. 8016: 493–500. <https://doi.org/10.1038/s41586-024-07487-w>.
- Allsopp, L. P., and P. Bernal. 2023. “Killing in the Name of: T6SS Structure and Effector Diversity.” *Microbiology* 169, no. 7: 001367. <https://doi.org/10.1099/mic.0.001367>.
- Alves, J. A., F. C. Leal, M. Previato-Mello, and J. F. d. S. Neto. 2022. “A Quorum Sensing-Regulated Type VI Secretion System Containing Multiple Nonredundant VgrG Proteins Is Required for Interbacterial Competition in *Chromobacterium violaceum*.” *Microbiology Spectrum* 10, no. 4: e0157622. <https://doi.org/10.1128/spectrum.01576-22>.
- Arnal, G., P. J. Stogios, J. Asohan, et al. 2019. “Substrate Specificity, Regiospecificity, and Processivity in Glycoside Hydrolase Family 74.” *Journal of Biological Chemistry* 294: 13233–13247. <https://doi.org/10.1074/jbc.RA119.009861>.
- Aschtgen, M.-S., M. S. Thomas, and E. Cascales. 2010. “Anchoring the Type VI Secretion System to the Peptidoglycan: TssL, TagL, TagP... What Else?” *Virulence* 1, no. 6: 535–540. <https://doi.org/10.4161/viru.1.6.13732>.
- Bachmann, V., B. Kostiuk, D. Unterweger, L. Diaz-Satizabal, S. Ogg, and S. Pukatzki. 2015. “Bile Salts Modulate the Mucin-Activated Type VI Secretion System of Pandemic *Vibrio cholerae*.” *PLoS Neglected Tropical Diseases* 9, no. 8: e0004031. <https://doi.org/10.1371/journal.pntd.0004031>.
- Beringer, J. E. 1974. “R Factor Transfer in *Rhizobium leguminosarum*.” *Microbiology* 84: 188–198. <https://doi.org/10.1099/00221287-84-1-188>.

- Bernal, P., L. P. Allsopp, A. Filloux, and M. A. Llamas. 2017. "The *Pseudomonas putida* T6SS Is a Plant Warden Against Phytopathogens." *ISME Journal* 11: 972–987. <https://doi.org/10.1038/ismej.2016.169>.
- Bernal, P., C. Civantos, D. Pacheco-Sánchez, J. M. Quesada, A. Filloux, and M. A. Llamas. 2023. "Transcriptional Organization and Regulation of the *Pseudomonas putida* K1 Type VI Secretion System Gene Cluster." *Microbiology* 169: 001295. <https://doi.org/10.1099/mic.0.001295>.
- Bernal, P., R. C. D. Furniss, S. Fecht, et al. 2021. "A Novel Stabilization Mechanism for the Type VI Secretion System Sheath." *Proceedings. National Academy of Sciences. United States of America* 118: e2008500118. <https://doi.org/10.1073/pnas.2008500118>.
- Bernal, P., M. A. Llamas, and A. Filloux. 2018. "Type VI Secretion Systems in Plant-Associated Bacteria." *Environmental Microbiology* 20: 1–15. <https://doi.org/10.1111/1462-2920.13956>.
- Bladergroen, M. R., K. Badelt, and H. P. Spaink. 2003. "Infection-Blocking Genes of a Symbiotic *Rhizobium leguminosarum* Strain That Are Involved in Temperature-Dependent Protein Secretion." *Molecular Plant-Microbe Interactions* 16: 53–64. <https://doi.org/10.1094/MPMI.2003.16.1.53>.
- Boratyn, G. M., C. Camacho, P. S. Cooper, et al. 2013. "BLAST: A More Efficient Report With Usability Improvements." *Nucleic Acids Research* 41: W29–W33. <https://doi.org/10.1093/nar/gkt282>.
- Borgeaud, S., L. C. Metzger, T. Scognari, and M. Blokesch. 2015. "The Type VI Secretion System of *Vibrio cholerae* Fosters Horizontal Gene Transfer." *Science* 347: 63–67. <https://doi.org/10.1126/science.1260064>.
- Boyer, F., G. Fichant, J. Berthod, Y. Vandenbrouck, and I. Attree. 2009. "Dissecting the Bacterial Type VI Secretion System by a Genome Wide In Silico Analysis: What Can Be Learned From Available Microbial Genomic Resources?" *BMC Genomics* 10: 1–14. <https://doi.org/10.1186/1471-2164-10-104>.
- Bromfield, E. S. P., and D. G. Jones. 1979. "The Competitive Ability and Symbiotic Effectiveness of Doubly Labelled Antibiotic Resistant Mutants of *Rhizobium trifolii*." *Annals of Applied Biology* 91: 211–219. <https://doi.org/10.1111/j.1744-7348.1979.tb06492.x>.
- Civantos, C., A. Ruiz, and P. Bernal. 2024. "A Robust Method to Perform In Vitro and In Planta Interbacterial Competition Assays: Killing Plant Pathogens by a Potent Biocontrol Agent." In *Host-Pathogen Interactions*, 115–129. Humana. https://doi.org/10.1007/978-1-0716-3617-6_8.
- De Campos, S. B., M. Lardi, A. Gandolfi, L. Eberl, and G. Pessi. 2017. "Mutations in Two Paraburkholderia Phymatum Type VI Secretion Systems Cause Reduced Fitness in Interbacterial Competition." *Frontiers in Microbiology* 8: 2473. <https://doi.org/10.3389/fmicb.2017.02473>.
- de Maagd, R., C. van Rossum, and B. J. Lugtenberg. 1988. "Recognition of Individual Strains of Fast-Growing Rhizobia by Using Profiles of Membrane Proteins and Lipopolysaccharides." *Journal of Bacteriology* 170, no. 8: 3782–3785. <https://doi.org/10.1128/jb.170.8.3782-3785.1988>.
- De Sousa, B. F. S., L. Domingo-Serrano, A. Salinero-Lanzarote, J. M. Palacios, and L. Rey. 2023. "The T6SS-Dependent Effector Re78 of *Rhizobium etli* Mim1 Benefits Bacterial Competition." *Biology* 12: 678. <https://doi.org/10.3390/biology12050678>.
- Dumont, B., L. Terradot, E. Cascales, L. Van Melder, and D. Jurénas. 2024. "Thioredoxin 1 Moonlights as a Chaperone for an Interbacterial ADP-Ribosyltransferase Toxin." *Nature Communications* 15: 10388. <https://doi.org/10.1038/s41467-024-54892-w>.
- Durán, D., P. Bernal, D. Vazquez-Arias, et al. 2021. "*Pseudomonas fluorescens* F113 Type VI Secretion Systems Mediate Bacterial Killing and Adaption to the Rhizosphere Microbiome." *Scientific Reports* 11: 1–13. <https://doi.org/10.1038/s41598-021-85218-1>.
- Durand, E., C. Cambillau, E. Cascales, and L. Journet. 2014. "VgrG, Tae, Tle, and Beyond: The Versatile Arsenal of Type VI Secretion Effectors." *Trends in Microbiology* 22: 498–507. <https://doi.org/10.1016/j.tim.2014.06.004>.
- Duxbury, Z., Y. Ma, O. J. Furzer, et al. 2016. "Pathogen Perception by NLRs in Plants and Animals: Parallel Worlds." *BioEssays* 38: 769–781. <https://doi.org/10.1002/bies.201600046>.
- Feng, F., and J.-M. Zhou. 2012. "Plant-Bacterial Pathogen Interactions Mediated by Type III Effectors." *Current Opinion in Plant Biology* 15: 469–476. <https://doi.org/10.1016/j.jpb.2012.03.004>.
- Figurski, D. H., and D. R. Helinski. 1979. "Replication of an Origin-Containing Derivative of Plasmid RK2 Dependent on a Plasmid Function Provided in Trans." *Proceedings of the National Academy of Sciences* 76: 1648–1652. <https://doi.org/10.1073/pnas.76.4.1648>.
- Finn, R. D., P. Coghill, R. Y. Eberhardt, et al. 2016. "The Pfam Protein Families Database: Towards a More Sustainable Future." *Nucleic Acids Research* 44: D279–D285.
- Gilchrist, C. L. M., and Y.-H. Chooi. 2021. "Clinker & Clustermap. Js: Automatic Generation of Gene Cluster Comparison Figures." *Bioinformatics* 37: 2473–2475. <https://doi.org/10.1093/bioinformatics/btab007>.
- González-Magaña, A., J. Altuna, M. Quera-Martín, et al. 2022. "The *P. aeruginosa* Effector Tse5 Forms Membrane Pores Disrupting the Membrane Potential of Intoxicated Bacteria." *Communications Biology* 5: 1–15. <https://doi.org/10.1038/s42003-022-04140-y>.
- Hachani, A., N. S. Lossi, A. Hamilton, et al. 2011. "Type VI Secretion System in *Pseudomonas aeruginosa*: Secretion and Multimerization of VgrG Proteins." *Journal of Biological Chemistry* 286: 12317–12327. <https://doi.org/10.1074/jbc.M110.193045>.
- Hachani, A., T. E. Wood, and A. Filloux. 2016. "Type VI Secretion and Anti-Host Effectors." *Current Opinion in Microbiology* 29: 81–93. <https://doi.org/10.1016/j.mib.2015.11.006>.
- Hespanhol, J. T., L. Nóbrega-Silva, and E. Bayer-Santos. 2023. "Regulation of Type VI Secretion Systems at the Transcriptional, Posttranscriptional and Posttranslational Level." *Microbiology* 169: 001376. <https://doi.org/10.1099/mic.0.001376>.
- Ho, B. T., T. G. Dong, and J. J. Mekalanos. 2014. "A View to a Kill: The Bacterial Type VI Secretion System." *Cell Host & Microbe* 15: 9–21. <https://doi.org/10.1016/j.chom.2013.11.008>.
- Hsu, F., S. Schwarz, and J. D. Mougous. 2009. "TagR Promotes PpkA-Catalysed Type VI Secretion Activation in *Pseudomonas aeruginosa*." *Molecular Microbiology* 72: 1111–1125. <https://doi.org/10.1111/j.1365-2958.2009.06701.x>.
- Hug, S., Y. Liu, B. Heiniger, et al. 2021. "Differential Expression of Paraburkholderia Phymatum Type VI Secretion Systems (T6SS) Suggests a Role of T6SS-b in Early Symbiotic Interaction." *Frontiers in Plant Science* 12: 699590. <https://doi.org/10.3389/fpls.2021.699590>.
- Hung, W., W.-N. Jane, and H. Wong. 2013. "Association of a d-Alanyl-d-Alanine Carboxypeptidase Gene With the Formation of Aberrantly Shaped Cells During the Induction of Viable but Nonculturable *Vibrio parahaemolyticus*." *Applied and Environmental Microbiology* 79: 7305–7312. <https://doi.org/10.1128/AEM.01723-13>.
- Jeffery, C. 1999. "Moonlighting proteins." *Trends in Biochemical Sciences* 24, no. 1: 8–11. [https://doi.org/10.1016/s0968-0004\(98\)01335-8](https://doi.org/10.1016/s0968-0004(98)01335-8).
- Jiménez-Guerrero, I., C. Medina, J. M. Vinardell, F. J. Ollero, and F. J. López-Baena. 2022. "The Rhizobial Type 3 Secretion System: The Dr. Jekyll and Mr. Hyde in the Rhizobium-Legume Symbiosis." *IJMS* 23: 11089. <https://doi.org/10.3390/ijms231911089>.
- Jiménez-Guerrero, I., N. Moreno-De Castro, and F. Pérez-Montañó. 2021. "One Door Closes, Another Opens: When Nodulation Impairment With Natural Hosts Extends Rhizobial Host-Range." *Environmental Microbiology* 23: 1837–1841. <https://doi.org/10.1111/1462-2920.15353>.
- Jiménez-Guerrero, I., F. Pérez-Montañó, J. A. Monreal, et al. 2015. "The Sinorhizobium (Ensifer) Fredii HH103 Type 3 Secretion System Suppresses Early Defense Responses to Effectively Nodulate Soybean."

- Molecular Plant-Microbe Interactions: MPMI* 28: 790–799. <https://doi.org/10.1094/MPMI-01-15-0020-R>.
- Kawaharada, Y., M. W. Nielsen, S. Kelly, et al. 2017. “Differential Regulation of the Epr3 Receptor Coordinates Membrane-Restricted Rhizobial Colonization of Root Nodule Primordia.” *Nature Communications* 8: 1–11. <https://doi.org/10.1038/ncomms14534>.
- Kelley, L. A., S. Mezulis, C. M. Yates, M. N. Wass, and M. J. E. Sternberg. 2015. “The Phyre2 Web Portal for Protein Modeling, Prediction and Analysis.” *Nature Protocols* 10: 845–858. <https://doi.org/10.1038/nprot.2015.053>.
- Khajanchi, B. K., J. Sha, E. V. Kozlova, et al. 2009. “N-Acylhomoserine Lactones Involved in Quorum Sensing Control the Type VI Secretion System, Biofilm Formation, Protease Production, and In Vivo Virulence in a Clinical Isolate of *Aeromonas hydrophila*.” *Microbiology* 155: 3518–3531. <https://doi.org/10.1099/mic.0.031575-0>.
- Krysciak, D., M. R. Orbegoso, C. Schmeisser, and W. R. Streit. 2015. “Molecular Keys to Broad Host Range in *Sinorhizobium fredii* NGR234, USDA257, and HH103.” In *Biological Nitrogen Fixation*, edited by F. J. de Bruijn, 325–336. <https://doi.org/10.1002/9781119053095.ch32>.
- Kumar, S., G. Stecher, and K. Tamura. 2016. “MEGA7: Molecular Evolutionary Genetics Analysis Version 7.0 for Bigger Datasets.” *Molecular Biology and Evolution* 33: 1870–1874. <https://doi.org/10.1093/molbev/msw054>.
- Lesic, B., M. Starkey, J. He, R. Hazan, and L. G. Rahme. 2009. “Quorum Sensing Differentially Regulates *Pseudomonas aeruginosa* Type VI Secretion Locus I and Homologous Loci II and III, Which Are Required for Pathogenesis.” *Microbiology* 155: 2845–2855. <https://doi.org/10.1099/mic.0.029082-0>.
- Lessard, I. A., and C. T. Walsh. 1999. “VanX, a Bacterial D-Alanyl-D-Alanine Dipeptidase: Resistance, Immunity, or Survival Function?” *Proceedings of the National Academy of Sciences* 96, no. 20: 11028–11032.
- Letunic, I., and P. Bork. 2016. “Interactive Tree of Life (iTOL) v3: An Online Tool for the Display and Annotation of Phylogenetic and Other Trees.” *Nucleic Acids Research* 44: W242–W245. <https://doi.org/10.1093/nar/gkw290>.
- Letunic, I., T. Doerks, and P. Bork. 2015. “SMART: Recent Updates, New Developments and Status in 2015.” *Nucleic Acids Research* 43: D257–D260. <https://doi.org/10.1093/nar/gku949>.
- Lin, H.-H., H.-M. Huang, M. Yu, E.-M. Lai, H.-L. Chien, and C.-T. Liu. 2018. “Functional Exploration of the Bacterial Type VI Secretion System in Mutualism: *Azorhizobium caulinodans* ORS571–*Sesbania Rostrata* as a Research Model.” *Molecular Plant-Microbe Interactions: MPMI* 31: 856–867. <https://doi.org/10.1094/MPMI-01-18-0026-R>.
- López-Baena, F., J. Ruiz-Sainz, M. Rodríguez-Carvajal, and J. Vinardell. 2016. “Bacterial Molecular Signals in the *Sinorhizobium fredii*-Soybean Symbiosis.” *International Journal of Molecular Sciences* 17: 755. <https://doi.org/10.3390/ijms17050755>.
- López-Baena, F. J., J. M. Vinardell, F. Pérez-Montaña, et al. 2008. “Regulation and Symbiotic Significance of Nodulation Outer Proteins Secretion in *Sinorhizobium fredii* HH103.” *Microbiology* 154: 1825–1836. <https://doi.org/10.1099/mic.0.2007/016337-0>.
- Ma, C., X. Zhang, X. Bao, and X. Zhu. 2024. “In the Symbiosome: Cross-Kingdom Dating Under the Moonlight.” *New Crops* 1: 100015. <https://doi.org/10.1016/j.ncrops.2024.100015>.
- Ma, L.-S., A. Hachani, J.-S. Lin, A. Filloux, and E.-M. Lai. 2014. “*Agrobacterium tumefaciens* Deploys a Superfamily of Type VI Secretion DNase Effectors as Weapons for Interbacterial Competition in Planta.” *Cell Host & Microbe* 16: 94–104. <https://doi.org/10.1016/j.chom.2014.06.002>.
- Mansfield, J. W. 2009. “From Bacterial Avirulence Genes to Effector Functions via the Hrp Delivery System: An Overview of 25 Years of Progress in Our Understanding of Plant Innate Immunity.” *Molecular Plant Pathology* 10: 721–734. <https://doi.org/10.1111/j.1364-3703.2009.00576.x>.
- Martinelli, F., F. J. Ollero, A. Giovino, et al. 2020. “Proposed Research for Innovative Solutions for Chickpeas and Beans in a Climate Change Scenario: The Mediterranean Basin.” *Sustainability* 12: 1315. <https://doi.org/10.3390/su12041315>.
- Miller, J. H. 1972. *Experiments in Molecular Genetics*. Cold Spring Harbor Laboratory.
- Mougous, J. D., M. E. Cuff, S. Raunser, et al. 2006. “A Virulence Locus of *Pseudomonas aeruginosa* Encodes a Protein Secretion Apparatus.” *Science* 312, no. 5779: 1526–1530.
- Mudgett, M. B. 2005. “New Insights to the Function of Phytopathogenic Bacterial Type III Effectors in Plants.” *Annual Review of Plant Biology* 56: 509–531. <https://doi.org/10.1146/annurev.arplant.56.032604.144218>.
- Nelson, M. S., and M. J. Sadowsky. 2015. “Secretion Systems and Signal Exchange Between Nitrogen-Fixing Rhizobia and Legumes.” *Frontiers in Plant Science* 6: 140795. <https://doi.org/10.3389/fpls.2015.00491>.
- Oldroyd, G. E. D. 2013. “Speak, Friend, and Enter: Signalling Systems That Promote Beneficial Symbiotic Associations in Plants.” *Nature Reviews in Microbiology* 11: 252–263. <https://doi.org/10.1038/nrmicr.20990>.
- Oldroyd, G. E. D., J. D. Murray, P. S. Poole, and J. A. Downie. 2011. “The Rules of Engagement in the Legume-Rhizobial Symbiosis.” *Annual Review of Genetics* 45: 119–144. <https://doi.org/10.1146/annurev-genet.110410.132549>.
- Pérez-Montaña, F., C. Aliás-Villegas, R. A. Bellogin, et al. 2014. “Plant Growth Promotion in Cereal and Leguminous Agricultural Important Plants: From Microorganism Capacities to Crop Production.” *Microbiological Research* 169: 325–336. <https://doi.org/10.1016/j.micres.2013.09.011>.
- Pérez-Montaña, F., I. Jiménez-Guerrero, P. Del Cerro, et al. 2014. “The Symbiotic Biofilm of *Sinorhizobium fredii* SMH12, Necessary for Successful Colonization and Symbiosis of *Glycine max* cv Osumi, Is Regulated by Quorum Sensing Systems and Inducing Flavonoids via NodD1.” *PLoS One* 9: e105901. <https://doi.org/10.1371/journal.pone.0105901>.
- Pfaffl, M. W. 2001. “A New Mathematical Model for Relative Quantification in Real-Time RT-PCR.” *Nucleic Acids Research* 29: e45–e45. <https://doi.org/10.1093/nar/29.9.e45>.
- Pissaridou, P., L. P. Allsopp, S. Wettstadt, S. A. Howard, D. A. I. Mavridou, and A. Filloux. 2018. “The *Pseudomonas aeruginosa* T6SS-VgrG1b Spike Is Topped by a PAAR Protein Eliciting DNA Damage to Bacterial Competitors.” *Proceedings of the National Academy of Sciences* 115: 12519–12524. <https://doi.org/10.1073/pnas.1814181115>.
- Pueppke, S. G., and W. J. Broughton. 1999. “Rhizobium Sp. Strain NGR234 and *R. fredii* USDA257 Share Exceptionally Broad, Nested Host Ranges.” *Molecular Plant-Microbe Interactions* 12: 293–318. <https://doi.org/10.1094/MPMI.1999.12.4.293>.
- Pukatzki, S., A. T. Ma, D. Sturtevant, et al. 2006. “Identification of a Conserved Bacterial Protein Secretion System in *Vibrio cholerae* Using the Dictyostelium Host Model System.” *Proceedings of the National Academy of Sciences* 103: 1528–1533. <https://doi.org/10.1073/pnas.0510322103>.
- Robertsen, B. K., P. Åman, A. G. Darvill, M. McNeil, and P. Albersheim. 1981. “Host-Symbiont Interactions: V. The Structure of Acidic Extracellular Polysaccharides Secreted by Rhizobium Leguminosarum and Rhizobium Trifolii.” *Plant Physiology* 67: 389–400. <https://doi.org/10.1104/pp.67.3.389>.
- Sabag-Daigle, A., J. L. Dyszel, J. F. Gonzalez, M. M. Ali, and B. M. M. Ahmer. 2015. “Identification of sdiA-Regulated Genes in a Mouse Commensal Strain of *Enterobacter cloacae*.” *Frontiers in Cellular and*

- Infection Microbiology* 5: 141829. <https://doi.org/10.3389/fcimb.2015.00047>.
- Salinero-Lanzarote, A., A. Pacheco-Moreno, L. Domingo-Serrano, et al. 2019. "The Type VI Secretion System of *Rhizobium etli* Mim1 Has a Positive Effect in Symbiosis." *FEMS Microbiology Ecology* 95: fiz054. <https://doi.org/10.1093/femsec/fiz054>.
- Samal, B., and S. Chatterjee. 2021. "Bacterial Quorum Sensing Facilitates *Xanthomonas Campestris* Pv. *Campestris* Invasion of Host Tissue to Maximize Disease Symptoms." *Journal of Experimental Botany* 72: 6524–6543. <https://doi.org/10.1093/jxb/erab211>.
- Sambrook, J., E. Fritsch, and T. Maniatis. 1989. *Molecular Cloning: A Laboratory Manual*. 2nd ed. Cold Spring Harbor Laboratory Press.
- Santin, Y. G., T. Doan, R. Lebrun, L. Espinosa, L. Journet, and E. Cascales. 2018. "In Vivo TssA Proximity Labelling During Type VI Secretion Biogenesis Reveals TagA as a Protein That Stops and Holds the Sheath." *Nature Microbiology* 3: 1304–1313. <https://doi.org/10.1038/s41564-018-0234-3>.
- Schindelin, J., C. T. Rueden, M. C. Hiner, and K. W. Eliceiri. 2015. "The ImageJ Ecosystem: An Open Platform for Biomedical Image Analysis." *Molecular Reproduction and Development* 82: 518–529. <https://doi.org/10.1002/mrd.22489>.
- Sievers, F., A. Wilm, D. Dineen, et al. 2011. "Fast, Scalable Generation of High-Quality Protein Multiple Sequence Alignments Using Clustal Omega." *Molecular Systems Biology* 7: 539. <https://doi.org/10.1038/msb.2011.75>.
- Simon, R. 1984. "High Frequency Mobilization of Gram-Negative Bacterial Replicons by the In Vitro Constructed Tn5-Mob Transposon." *Molecular & General Genetics* 196: 413–420. <https://doi.org/10.1007/BF00436188>.
- Spaink, H. P., R. J. H. Okker, C. A. Wijffelman, E. Pees, and B. J. J. Lugtenberg. 1987. "Promoters in the Nodulation Region of the *Rhizobium leguminosarum* Sym Plasmid pRL1J1." *Plant Molecular Biology* 9: 27–39. <https://doi.org/10.1007/BF00017984>.
- Staehelin, C., and H. B. Krishnan. 2015. "Nodulation Outer Proteins: Double-Edged Swords of Symbiotic Rhizobia." *Biochemical Journal* 470: 263–274. <https://doi.org/10.1042/BJ20150518>.
- Tighilt, L., F. Boulila, B. F. S. De Sousa, et al. 2022. "The Bradyrhizobium Sp. LmicA16 Type VI Secretion System Is Required for Efficient Nodulation of *Lupinus* Spp." *Microbial Ecology* 84: 844–855. <https://doi.org/10.1007/s00248-021-01892-8>.
- Van Kempen, M., S. S. Kim, C. Tumescheit, et al. 2024. "Fast and Accurate Protein Structure Search With Foldseek." *Nature Biotechnology* 42: 243–246. <https://doi.org/10.1038/s41587-023-01773-0>.
- Vidal, J., G. Godbillon, and P. Gadal. 1980. "Recovery of Active, Highly Purified Phosphoenolpyruvate Carboxylase From Specific Immunoabsorbent Column." *FEBS Letters* 118: 31–34. [https://doi.org/10.1016/0014-5793\(80\)81211-7](https://doi.org/10.1016/0014-5793(80)81211-7).
- Vincent, J. M. 1970. *A Manual for the Practical Study of Root-Nodule Bacteria*, 144–145. Blackwell Scientific Publications.
- Walker, T. S., H. P. Bais, E. Grotewold, and J. M. Vivanco. 2003. "Root Exudation and Rhizosphere Biology." *Plant Physiology* 132: 44–51. <https://doi.org/10.1104/pp.102.019661>.
- Weber, B. S., S. W. Hennon, M. S. Wright, et al. 2016. "Genetic Dissection of the Type VI Secretion System in *Acinetobacter* and Identification of a Novel Peptidoglycan Hydrolase, TagX, Required for Its Biogenesis." *MBio* 7: e01253-16. <https://doi.org/10.1128/mbio.01253-16>.
- Winzer, K., and P. Williams. 2001. "Quorum Sensing and the Regulation of Virulence Gene Expression in Pathogenic Bacteria." *International Journal of Medical Microbiology* 291: 131–143. <https://doi.org/10.1078/1438-4221-00110>.
- Wu, H.-Y., P.-C. Chung, H.-W. Shih, S.-R. Wen, and E.-M. Lai. 2008. "Secretome Analysis Uncovers an Hcp-Family Protein Secreted via a Type VI Secretion System in *Agrobacterium tumefaciens*." *Journal of Bacteriology* 190: 2841–2850. <https://doi.org/10.1128/jb.01775-07>.
- Yu, N. Y., J. R. Wagner, M. R. Laird, et al. 2010. "PSORTb 3.0: Improved Protein Subcellular Localization Prediction With Refined Localization Subcategories and Predictive Capabilities for all Prokaryotes." *Bioinformatics* 26: 1608–1615. <https://doi.org/10.1093/bioinformatics/btq249>.
- Zaat, S. A., C. A. Wijffelman, H. P. Spaink, A. A. van Brussel, R. J. Okker, and B. J. Lugtenberg. 1987. "Induction of the nodA Promoter of *Rhizobium leguminosarum* Sym Plasmid pRL1J1 by Plant Flavanones and Flavones." *Journal of Bacteriology* 169: 198–204. <https://doi.org/10.1128/jb.169.1.198-204.1987>.
- Zheng, J., O. S. Shin, D. E. Cameron, and J. J. Mekalanos. 2010. "Quorum Sensing and a Global Regulator TsrA Control Expression of Type VI Secretion and Virulence in *Vibrio cholerae*." *Proceedings of the National Academy of Sciences* 107: 21128–21133. <https://doi.org/10.1073/pnas.1014998107>.
- Zipfel, C., and G. E. D. Oldroyd. 2017. "Plant Signalling in Symbiosis and Immunity." *Nature* 543: 328–336. <https://doi.org/10.1038/nature22009>.

Supporting Information

Additional supporting information can be found online in the Supporting Information section.